D1-82-0427

BOEING SCIENTIFIC RESEARCH LABORATORIES

An Experimental Investigation of Mass Flow Through Short Circular Tubes in the Transition Flow Regime

A.K. Sreekanth

April 1965

D1-82-0427

BOEING SCIENTIFIC RESEARCH LABORATORIES

FLIGHT SCIENCES LABORATORY REPORT NO. 95

AN EXPERIMENTAL INVESTIGATION OF MASS FLOW THROUGH SHORT CIRCULAR TUBES IN THE TRANSITION FLOW REGIME

by

A. K. Sreekanth

April 1965

AN EXPERIMENTAL INVESTIGATION OF MASS FLOW THROUGH SHORT CIRCULAR TUBES IN THE TRANSITION FLOW REGIME

A. K. Sreekanth

Boeing Scientific Research Laboratories, Seattle, Washington

ABSTRACT

The mass flow of nitrogen gas through short circular tubes was measured in the transition flow regime with the length-to-diameter ratios varied between 0.005 and 1 and with pressure ratios across the tubes varied between 1 and 20. The range of Knudsen numbers (ratio of upstream mean free path to the diameter of the tube) covered was between 0.1 to 1.7. Comparisons are made of the measurements with existing theories, and a semi-empirical equation is developed to correlate the measured data at all of the pressure ratios, Knudsen numbers, and length-to-diameter ratios covered in the present study.

TABLE OF CONTENTS

BLANK PAGE

I. INTRODUCTION

The theoretical and experimental investigation of the flow of a rarefied gas through tubes had its origin more than fifty years ago when Knudsen studied the flow of pure gases in long circular tubes. He derived a theoretical expression for the mass flow under free molecular flow conditions and from an experimental study deduced a semi-empirical formula for the transition from molecular to Poiseuille flow. A few years later, Clausing theoretically investigated flow through short tubes under free molecular conditions. Almost all of the experimental work done since on the flow of rarefied gases through tubes has been confined to very low pressure ratios across the tube, although considerable amount of work has been done recently at high pressure ratios for convergent-divergent nozzles using nitrogen[1] and argon[2]. Mass flow studies at very high pressure ratios have also been done through short tubes using cesium gas[3]. Liepmann[4] investigated the transition flow through a circular orifice at extremely high pressure ratios to check the near free molecular flow theory being developed at that time. Liepmann's work was extended recently[5] to low and moderate pressure ratios. The present work is an extension of the orifice flow study, in which the thickness of the orifice is gradually increased to result in a short tube.

II. EXPERIMENTAL ARRANGEMENT AND MEASUREMENTS

Apparatus

All the experiments were conducted in the Boeing Scientific Research Laboratories' continuous flow, low density gas dynamics facility. It consists of a large stainless steel vacuum tank, 44" in diameter and 108" long, one end of which is connected to a large vapor booster pump (*Edwards* 18 B 4) which has a rated unbaffled pumping speed of 2800 liters per second at 10^{-3} Torr. An orifice plate or a short tube separates this tank into upstream and downstream chambers (Fig. 1). Nitrogen gas at room temperature (22.5°C) is admitted into the upstream chamber through a mass-flow transducer and a throttle valve. Downstream pressure is controlled by the vacuum pump and an adjustable leak. The pressures in the two chambers are measured and monitored by two sets of thermistor gauges calibrated against a precision mercury McLeod gauge.

Mass Flow Transducers

Commercially available *Hastings-Raydist* mass-flow transducers, with slight modifications for increased accuracy, were used to measure the mass flow. Two sets of transducers were used, one having a range of 0 - 20 standard cc/min. and the other 0 - 100 standard cc/min. The output of the transducers were read on a precision (Laboratory Standard) millivolt recorder, and the mass-flow meters were calibrated both before and after the experiments against a precision primary standard *Porter* low-flow calibrator.

Short Tubes

Holes of 1" diameter drilled in 18" diameter flat aluminum plates

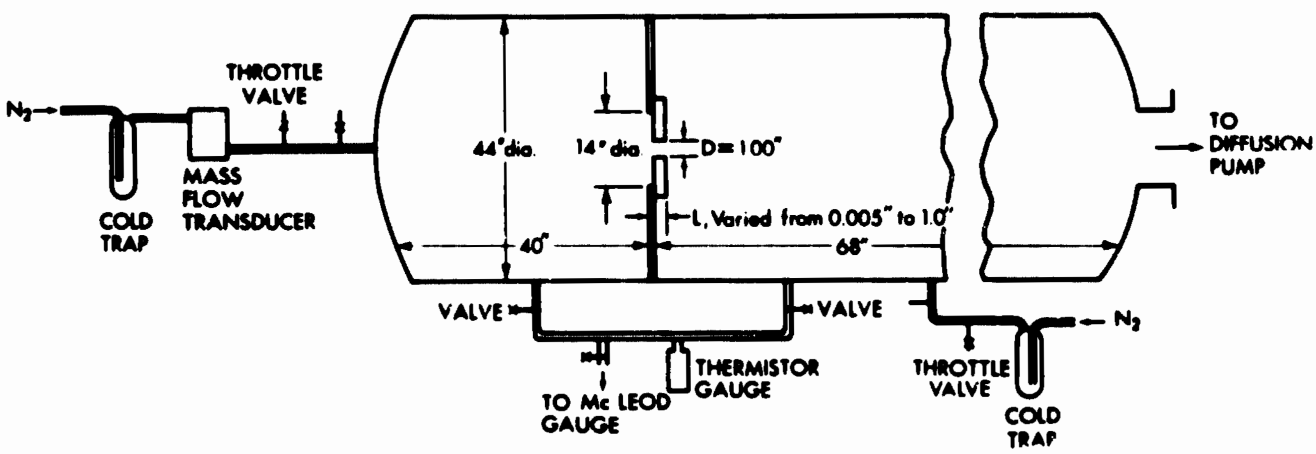

Figure 1. Schematic diagram of the experimental apparatus.

of various thicknesses were used as short tubes. Four geometries were tested. All had the same diameter of one inch, but the lengths were 0.233, 0.493, 0.756, and 0.995 inches. The orifice plate consisted of a circular hole, again one inch in diameter drilled in a 0.005" thick copper sheet epoxied to a brass ring of 12" inside diameter. The short tube and orifice plates were fitted with "O" ring seals into the dividing wall in the tank. The sizes of the vacuum tank and the orifice and short tube plates were such that for all practical purposes one could consider them as being in an infinite plane wall separating two large chambers.

Using nitrogen at room temperature (22.5°C) the mass flow through tubes and orifice was measured for various upstream and downstream pressure conditions. For each of the tubes the mass flows were measured at five Knudsen number values, 0.124; 0.247; 0.494; 0.986; and 1.69. (The Knudsen number in this case is defined as the ratio of upstream mean free path to the diameter of the tube or orifice.) For each Knudsen number the range of pressure ratios covered varied from 1 to 20. The upstream pressures were kept constant at 15.9, 7.96, 3.98, 1.99, and 1.16 microns Hg. pressures, corresponding to the above Knudsen number values, and only the downstream pressure was changed to obtain the various pressure ratio conditions. Some measurements were also taken at an upstream pressure of 23.8 microns Hg, corresponding to a Knudsen number of 0.083 for small pressure ratios across the tube or orifice.

III. ACCURACY

The pressure readings were accurate to ± 1%, corresponding to the absolute accuracy of the McLeod gauge used for calibrating the thermistor gauges. In the pressure range of the present experiments, the output of the thermistor vs. pressure is linear. Since the same pair of thermistors was used to measure both upstream and downstream pressures, the ratio of millivolt outputs should then represent the pressure ratios and the uncertainty therein was within ± ½%. For flow rates greater than 3.0 standard cc/min. the flow readings were accurate within ± 1½%. For lower flow rates, it is probable that the error might be as high as ± 3% of its absolute value. Repeatability of the experiments was within ± 1%.

IV. RESULTS AND DISCUSSION

The plots of the flow rate per unit cross-sectional area of the tube vs. pressure ratios at various Knudsen number ranges for all of the tube geometries tested are shown in Figures 2 to 6. Referring to these figures, it can be observed that at a Knudsen number of 0.12 the flow rate is still increasing at pressure ratios as high as 20. Liepmann[4] has pointed out that for the case of the flow of a continuum gas through a circular aperture, the pressure ratio required to choke the flow is one or two orders of magnitude greater than for a convergent-divergent (Laval) nozzle. The same argument can be extended to the case of short tubes in which, due to small length-to-diameter ratios, the flow through them is still like an orifice-type flow. If one assumes that the flow is still behaving as a continuum-type flow at $Kn = 0.12$, the present experiments substantiate the fact that pressure ratios required to choke the flow in orifices and short tubes are very much higher than for a Laval nozzle.

For the calculation of the Knudsen number, the mean free path was determined by the following relation

$$\lambda = \frac{16\mu}{5P_1} \sqrt{\frac{RT_1}{2\pi}} \quad . \tag{1}$$

The value of the viscosity, μ, used was $1760 \cdot 4 \times 10^{-7}$ poise, corresponding to a temperature of $22.5^{\circ}C$.

Figure' 7 to 11 show plots of nondimensionalized mass flow vs. pressure ratios at various Knudsen numbers. The nondimensionalized quantities $\dot{m}/\dot{m}_{fm}$ were obtained by dividing the measured mass flow rate by the theoretical free molecule flow rate, which in turn is obtained by multiplying the theoretical orifice free molecule efflux rate by the appropriate

Clausing factor,

$$\dot{m}_{fm} = \frac{1}{\sqrt{2\pi RT}} A(P_1 - P_2)\, k \qquad (2)$$

where A = cross sectional area of the tube; k = Clausing factor. It is assumed that the temperature of the gas is the same on either side of the tube or orifice and that the reflection of molecules from tube walls is completely diffuse. The Clausing factors were obtained by interpolating between the values given in Demarcus' report[6]. For tube geometries used in the present experiments, the Clausing factors used are listed in Table I.

TABLE I

Values of Clausing Factor for Tube Geometries
Used in the Experiment

Length/Diameter	Clausing Factor, k
0.9946	0.5515
0.7562	0.5797
0.4926	0.6752
0.2325	0.8125
0.005	0.9952

Cross plots of $\dot{m}/\dot{m}_{fm}$ vs. Kn at different pressure ratios are presented in Figs. 12 to 16. Tables 2 through 31 list the mass flow data. It can be seen from these plots that at low Knudsen numbers the deviation from the free molecular flow values is greater at lower pressure ratios and gradually decreases as pressure ratio is increased. At high Knudsen numbers the deviation becomes almost constant at all pressure ratios for a given Knudsen number. It was also observed from measurements that the $\dot{m}/\dot{m}_{fm}$ value decreases slightly as the length of the tube is increased for the same diameter at all Knudsen numbers and pressure ratios. Graphs illustrating this effect at pressure ratios of 17, 10, 5, 3, and 2 are shown in Figures 17 to 21. The scatter in the $\dot{m}/\dot{m}_{fm}$ at high Knudsen numbers for pressure ratios close to one in Figures 7 to 11 is probably due to the fact that theoretical $\dot{m}_{fm}$ were calculated by the pressure difference $(P_1 - P_2)$ across the tube for a given pressure ratio; since we are subtracting two quantities of equal magnitude, a very slight error in the pressure ratio readings will be magnified in the pressure difference. (The present results of $\dot{m}/\dot{m}_{fm}$ for the orifice differ by 2 - 3% from those reported earlier[5]. This difference is attributed to the slight uncertainty involved in the measurement of the pressures. In the earlier work the thermistor gauges were calibrated against a commercially available McLeod gauge. The absolute accuracy of this gauge was found to be not as good as that of a primary standards McLeod gauge against which the thermistor gauges were calibrated in the present runs and mass flow measurements repeated.)

For the creeping flow (flow in which the inertia terms can be neglected in comparison to viscous terms in the Navier-Stokes equation) of a continuum gas through a circular orifice, Roscoe[7] has shown that the pressure drop is related to volumetric flow, Q, by the relation

$$\Delta P = 24 \frac{Q\mu}{D^3} \qquad (3)$$

where μ is the viscosity of the gas and D the diameter of the orifice.

A similar expression relating the pressure drop to flow rate has been obtained by Weissberg[8] for short tubes

$$\Delta P = \frac{24 Q \mu}{D^3} \left[1 + \frac{16}{3\pi} \frac{L}{D} \right] \quad (4)$$

where L = length of the tube. Both the equations (3) and (4) show that for a fixed L and D the pressure drop is linearly proportional to the volumetric flow. For the case of free molecule flow, the relation between pressure drop and flow rate is

$$\frac{Q \mu}{\Delta P D^3} = 0.245\ k \cdot Kn \quad (5)$$

where Kn = Knudsen number based on diameter and k the Clausing factor, Q, μ, and Kn values being evaluated at upstream conditions. (For the derivation of the above equation the relationship between viscosity and the mean free path as given by Equation (1) was used.)

From the measurements it was found that in the transition flow, for pressure ratios less than about 1.2, the flow rate was directly proportional to the pressure drop but the proportionality constant was a function of Knudsen number and tube geometry. This is shown in Figure 22. For the determination of the quantity Q/ΔP, the measured flow rates as a function of pressure ratios were plotted and a smooth curve was drawn through the experimental points. From this curve a cross plot of Q vs ΔP was made and the quantity Q/ΔP was determined. Table 32 lists the values thus obtained for various tube geometries and Knudsen numbers. A semi-empirical equation which was developed (see below) to correlate with the mass flow measurements was also found to fit fairly well with the measured flow rate at extremely low pressure ratios, as shown in Figure 23. The empirical equation is valid only in the transition or near free molecule flow regimes.

Willis[9] has theoretically analyzed the mass flow through a circular orifice at very high pressure ratios in the near free molecule flow regime. His final calculations are restricted to one iteration in an integral iteration scheme. Comparison of this result with the orifice data at a pressure ratio of 17 is shown in Figure 24. The theory underestimates the mass flow slightly for Reynolds number, $Re = \left(\frac{DP_1}{\sqrt{RT_1}\,\mu_1}\right)$ less than one. As pointed out by Willis there is no reason to expect the first iterate solution to agree with data for Re > 1 since further iterations are then necessary. Although comparison is made of the experimental data at a pressure ratio of 17 with the theory which assumes infinite or very large pressure ratio across the orifice, the $\dot{m}/\dot{m}_{fm}$ values for high Knudsen numbers have almost become independent of pressure ratios from 5 to 17 (Figure 7) and it is therefore reasonable to assume that the same values hold good for larger pressure ratios.

Milligan[2] in his work on nozzle characteristics in the transition regime did some experiments on the flow through a short tube of L/D = 0.312. His plot of C_D vs. D/2λ show very little dependence of C_D on the pressure ratios 2 to 20 over the entire transition flow regime. (C_D = discharge coefficient, defined as the ratio of actual mass flow to one-dimensional isentropic mass flow for choked conditions

$$C_D = \frac{\dot{m}_{meas}}{\dot{m}_{isen}} = \frac{\dot{m}_{meas}}{\left[\frac{\gamma}{R}\left(\frac{2}{\gamma+1}\right)^{\frac{\gamma+1}{\gamma-1}}\right]^{\frac{1}{2}}\left[\frac{P_1}{T_1}A\right]} \qquad (6)$$

where γ is the ratio of specific heats, R = the gas constant, A = cross sectional area of the tube. The subscripts 1 refer to upstream conditions.)

Figure 25 is a plot of the present results for a short tube of L/D = 0.233. The abscissa and ordinate have the same meaning as described above. The plot shows a very significant dependence on the pressure ratios in the transition regime, an observation contrary to those of Milligan.

The Poiseuille formula for the mass flow for long circular tubes with slip boundary conditions is

$$\dot{m} = \left[\frac{\pi D^4}{128\ \mu RT}\ \bar{P}\ \frac{\Delta P}{L} + \frac{0.519\ D^3}{\bar{c}}\ \frac{\Delta P}{L}\right] \tag{7}$$

where $\bar{P} = \frac{P_1 + P_2}{2}$ and $\Delta P = P_1 - P_2$, μ = viscosity of the gas, $\bar{c}$ = average molecular velocity, L = length of the tube.

The above equation is similar to that given in Present's book[10] except that it is modified by the use of Equation (1) for the relation between viscosity and mean free path.

From the measurements it was found that for a given Knudsen number, based on upstream conditions and tube diameter, the decrease in mass flow as the tube length was increased was proportional to L(1+D/L), at all of the pressure ratios. It was also observed that these measured values could be well correlated with Equation (7) when the equation was multiplied by a factor (L/L+D). The modified Poiseuille equation is

$$\dot{m} = \left[\frac{\pi D^4}{128\ \mu RT}\ \bar{P}\ \Delta P + \frac{0.519\ D^3}{\bar{c}}\ \Delta P\right] \frac{1}{L(1+D/L)} \quad . \tag{8}$$

This semi-empirical equation will predict the mass flow fairly well for all pressure ratios, for the range of Knudsen numbers and L/D ratios covered in the present experiment when the viscosity and temperature are evaluated at upstream conditions.

The comparison between the measured values and the Equation (8) are shown in Figures 26 to 30. The ordinate represents the volumetric flow per unit cross sectional area of the tube or orifice times L(1+D/L). The solid line represents Equation (8) converted into proper units plotted in the graphs. It could be seen that the agreement is very good at high Knudsen numbers, and as the Knudsen number is decreased the semi-empirical theory overestimates the mass flow by 5% at high pressure ratios. Although the experiments were done at a fixed diameter of 1" for all the tubes and orifice, the semi-empirical relation developed will be valid for other diameters as well since Equation (8) can be converted with a little algebra to

$$\dot{m}/\text{unit area} = \frac{(P_1 - P_2)}{2\sqrt{2\pi RT_1}\,(1+L/D)}\left[\frac{1+P_2/P_1}{10\ Kn} + 2.076\right]. \qquad (9)$$

Thus for a given Knudsen number, L/D, and pressure ratio, the ratio of mass flow per unit cross-sectional area is independent of the diameter of the tube. The ratio of mass flow as given by the Equation (9) to the theoretical free molecule flow value is

$$\frac{\dot{m}}{\dot{m}_{fm}} = \frac{1}{2k(1+L/D)}\left[2.076 + \frac{1+P_2/P_1}{10\ Kn}\right]. \qquad (10)$$

(k = Clausing factor)

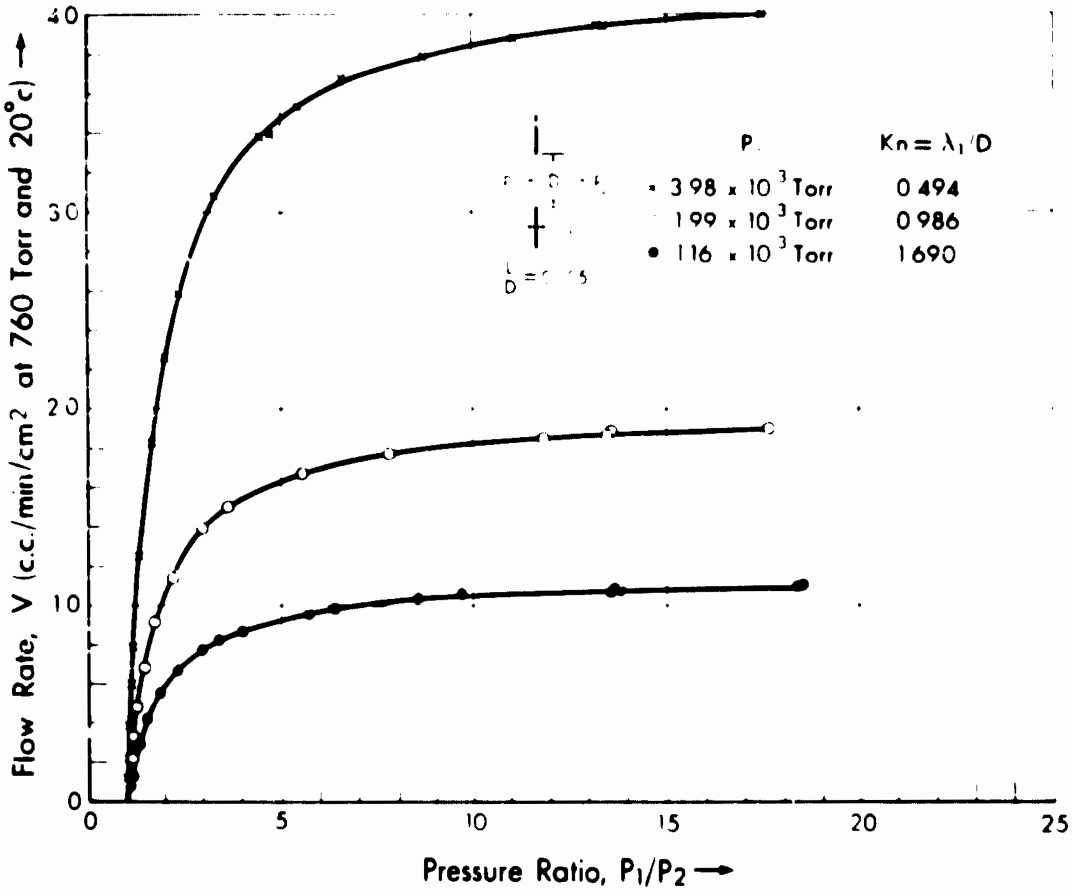

Figure 2(a). Flow rate at various pressure ratios for an orifice ($\frac{L}{D}$ = 0.005).

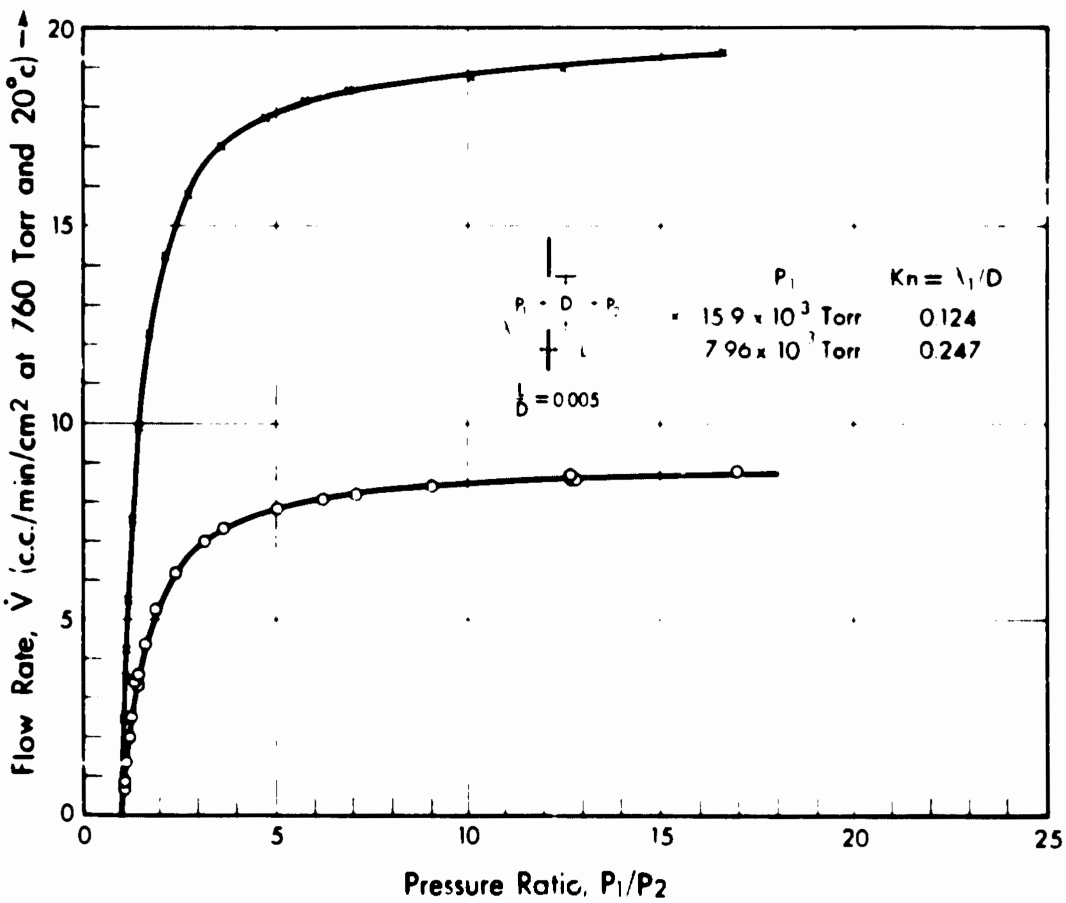

Figure 2(b). Flow rate at various pressure ratios for an orifice ($\frac{L}{D}$ = 0.005).

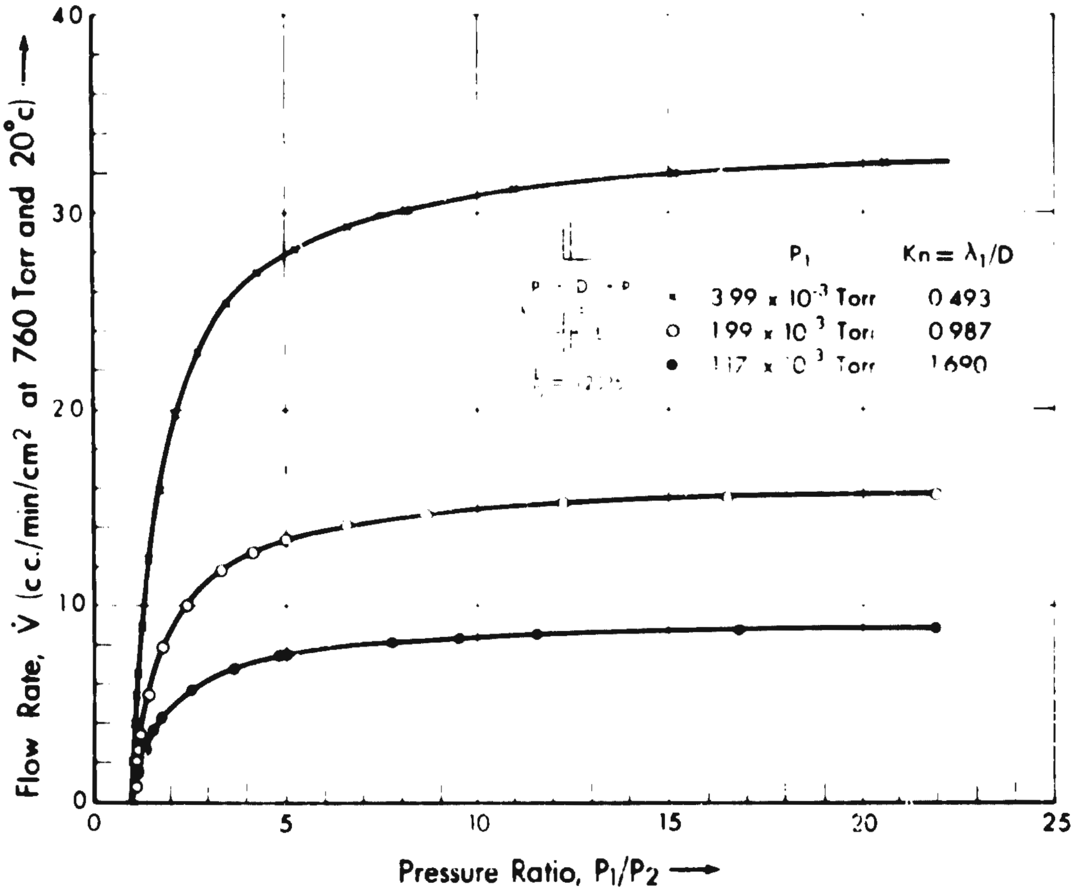

Figure 3(a). Flow rate at various pressure ratios for a short tube having a length to diameter ratio of 0.233.

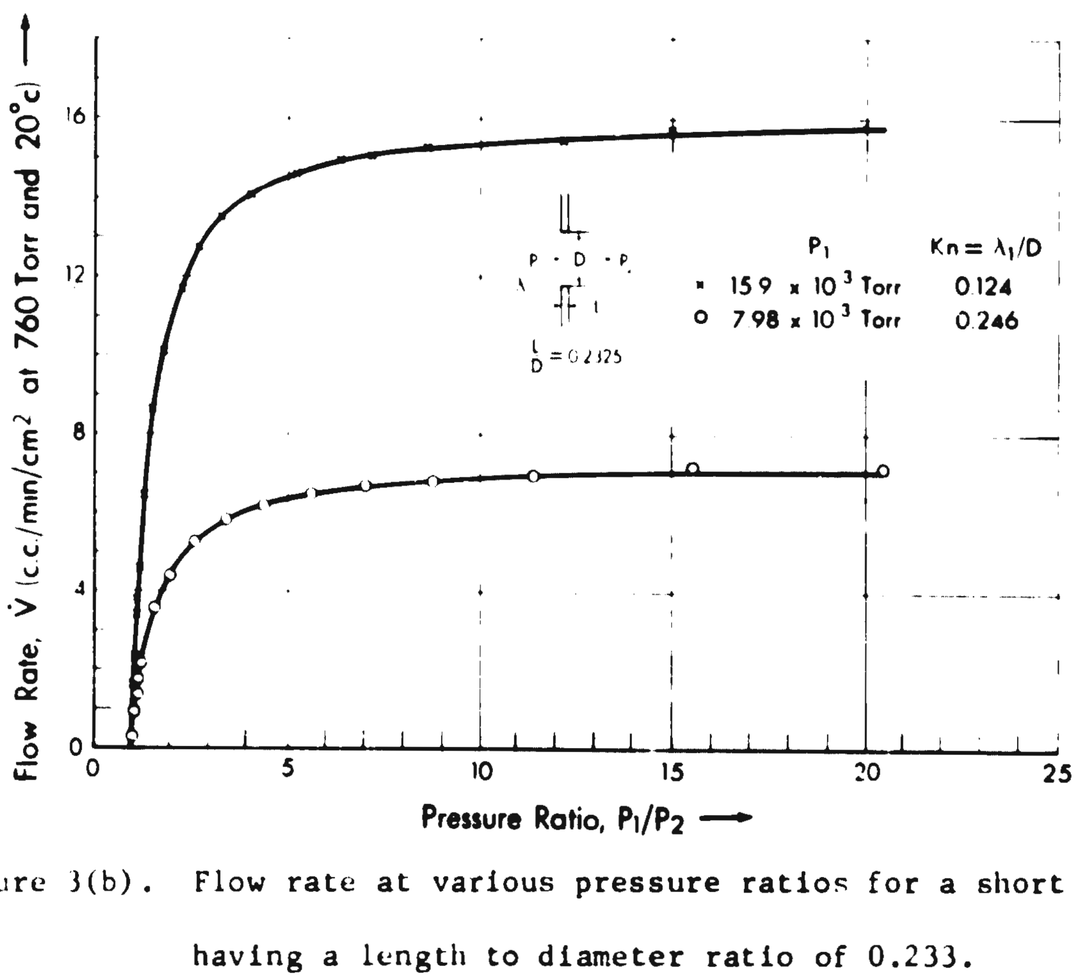

Figure 3(b). Flow rate at various pressure ratios for a short tube having a length to diameter ratio of 0.233.

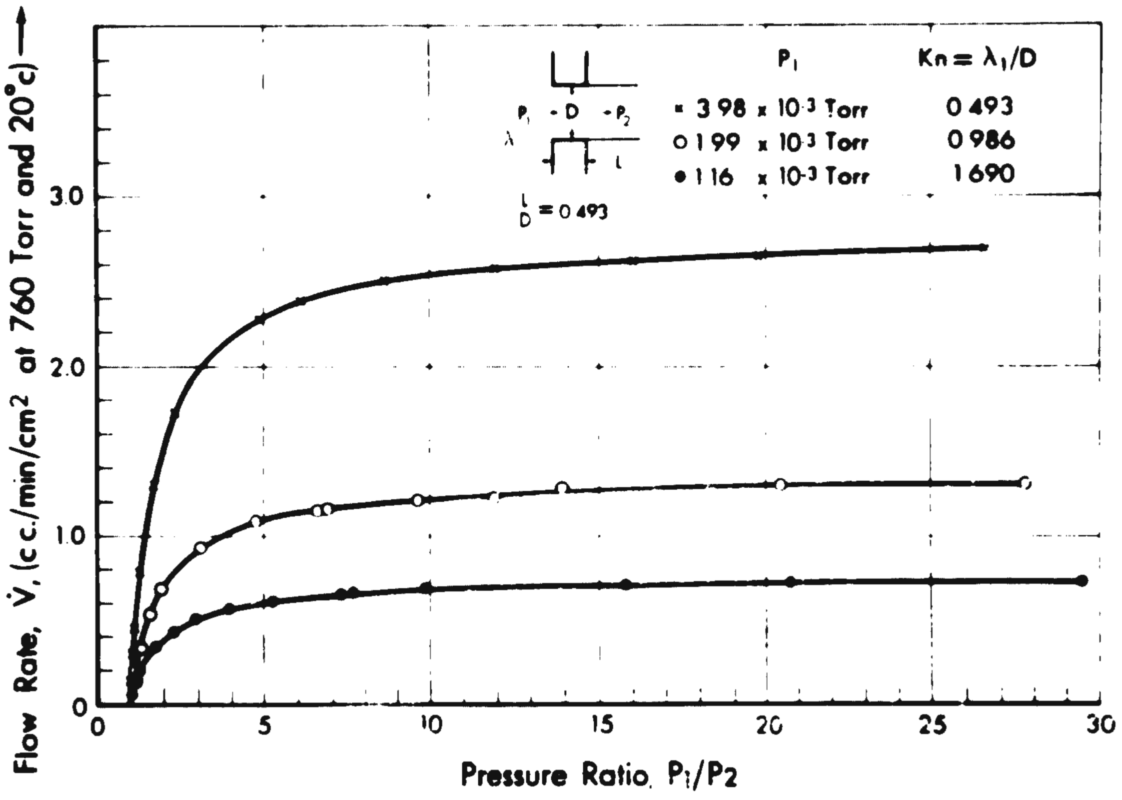

Figure 4(a). Flow rate at various pressure ratios for a short tube having a length to diameter ratio of 0.493.

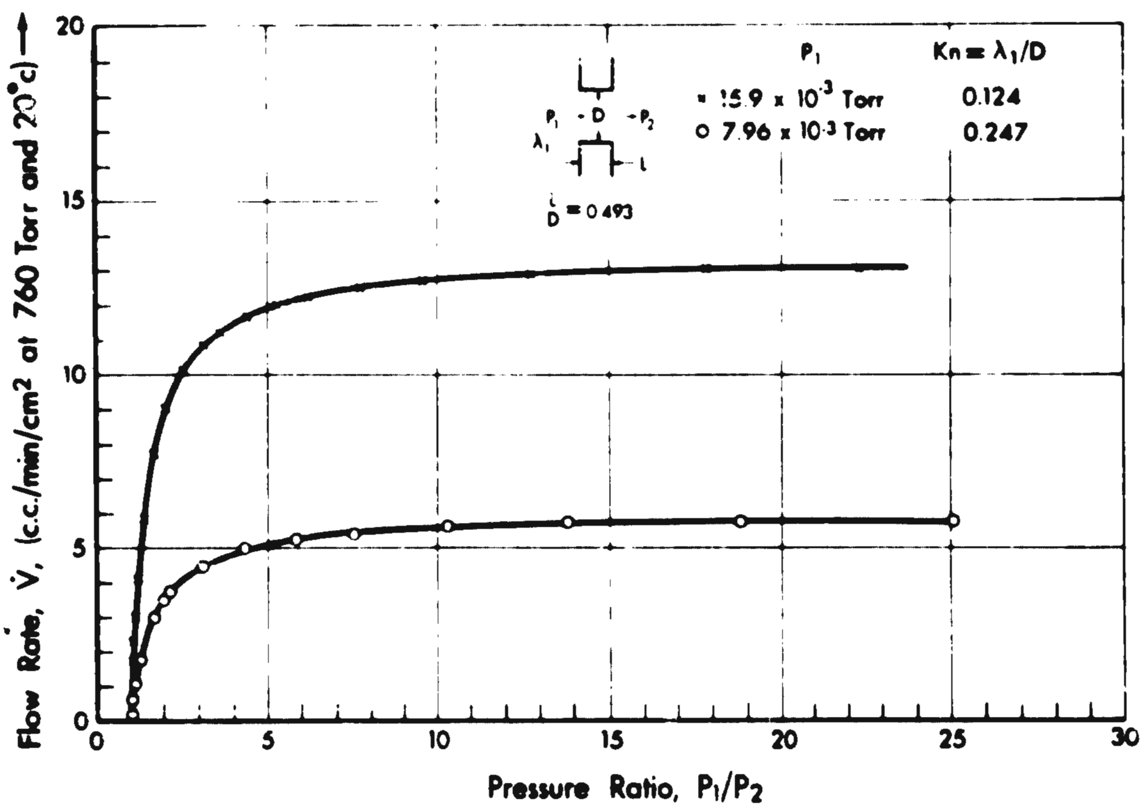

Figure 4(b). Flow rate at various pressure ratios for a short tube having a length to diameter ratio of 0.493.

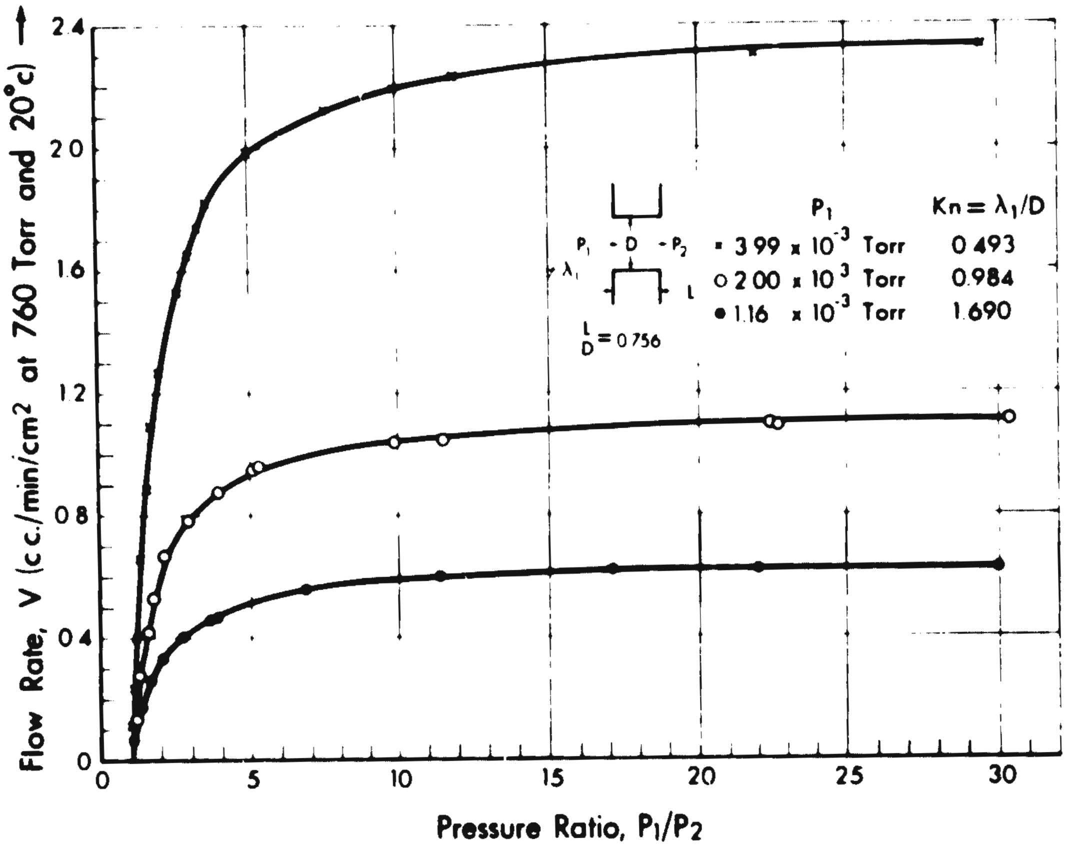

Figure 5(a). Flow rate at various pressure ratios for a short tube having a length to diameter ratio of 0.756.

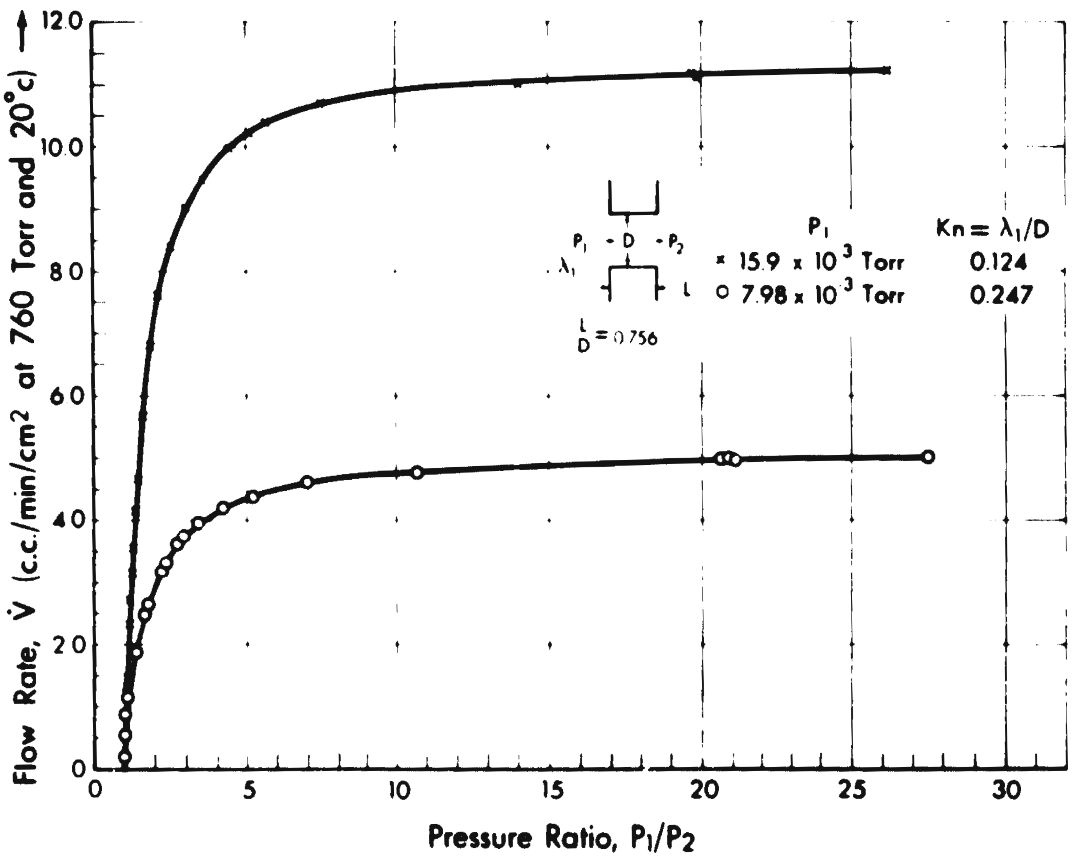

Figure 5(b). Flow rate at various pressure ratios for a short tube having a length to diameter ratio of 0.756.

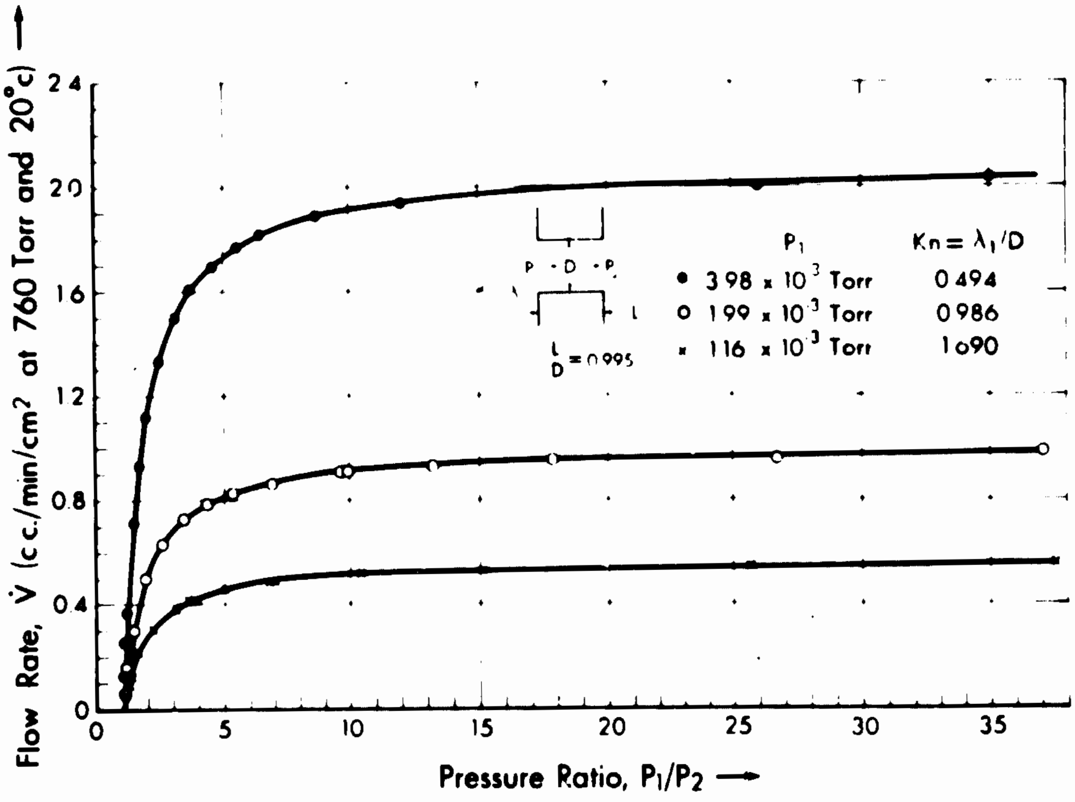

Figure 6(a). Flow rate at various pressure ratios for a short tube having a length to diameter ratio of 0.995.

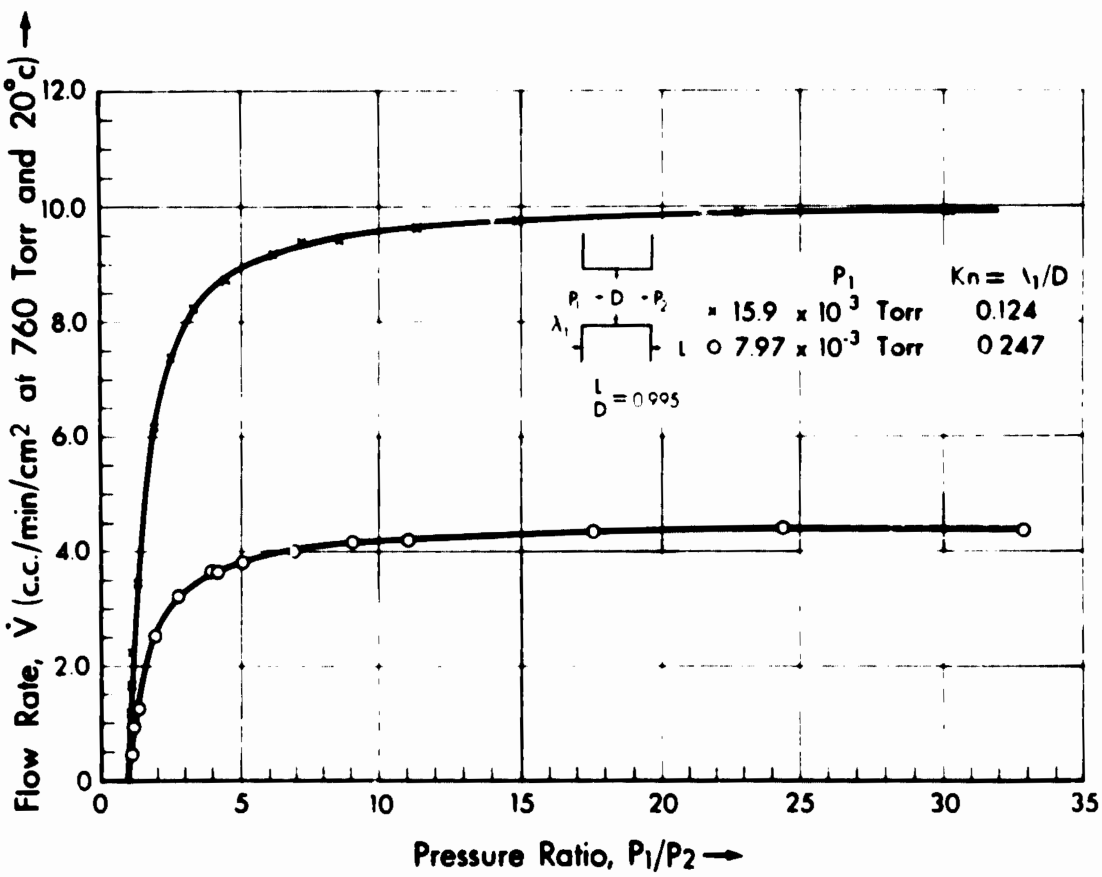

Figure 6(b). Flow rate at various pressure ratios for a short tube having a length to diameter ratio of 0.995.

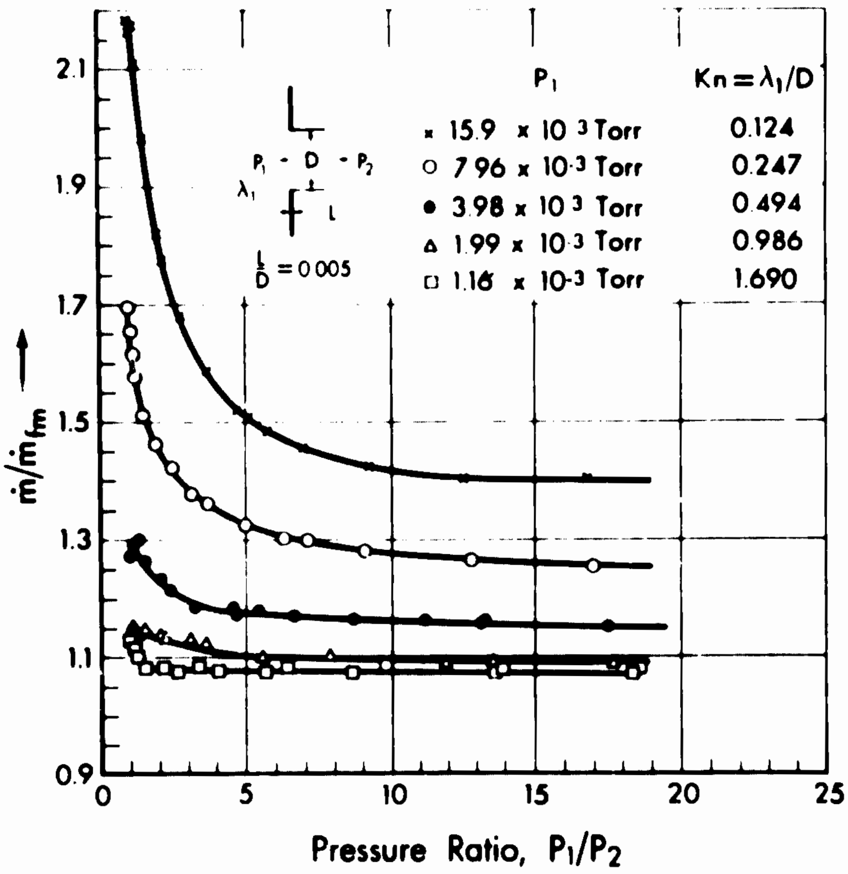

Figure 7. Nondimensionalized mass flow vs pressure ratio at various Knudsen numbers for an orifice ($\frac{L}{D}$ = 0.005).

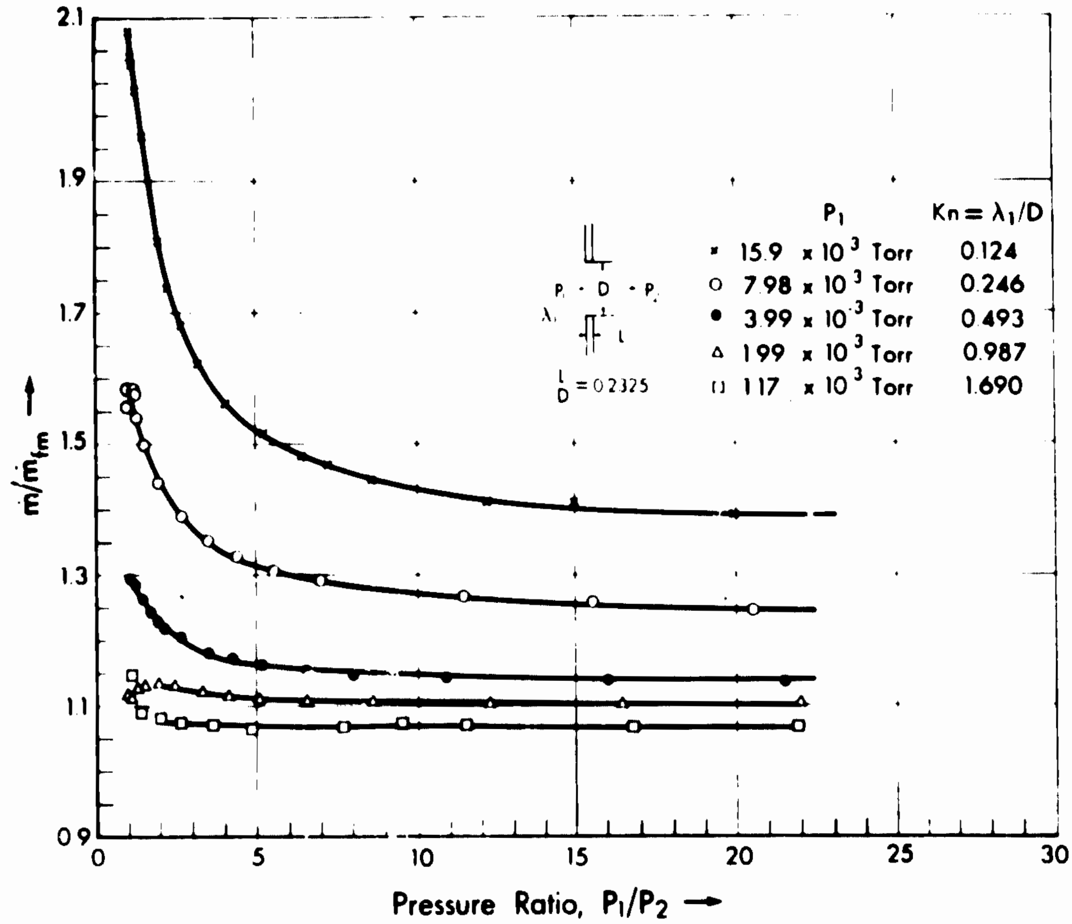

Figure 8. Nondimensionalized mass flow vs pressure ratio at various Knudsen numbers for a short tube, $\frac{L}{D}$ = 0.233.

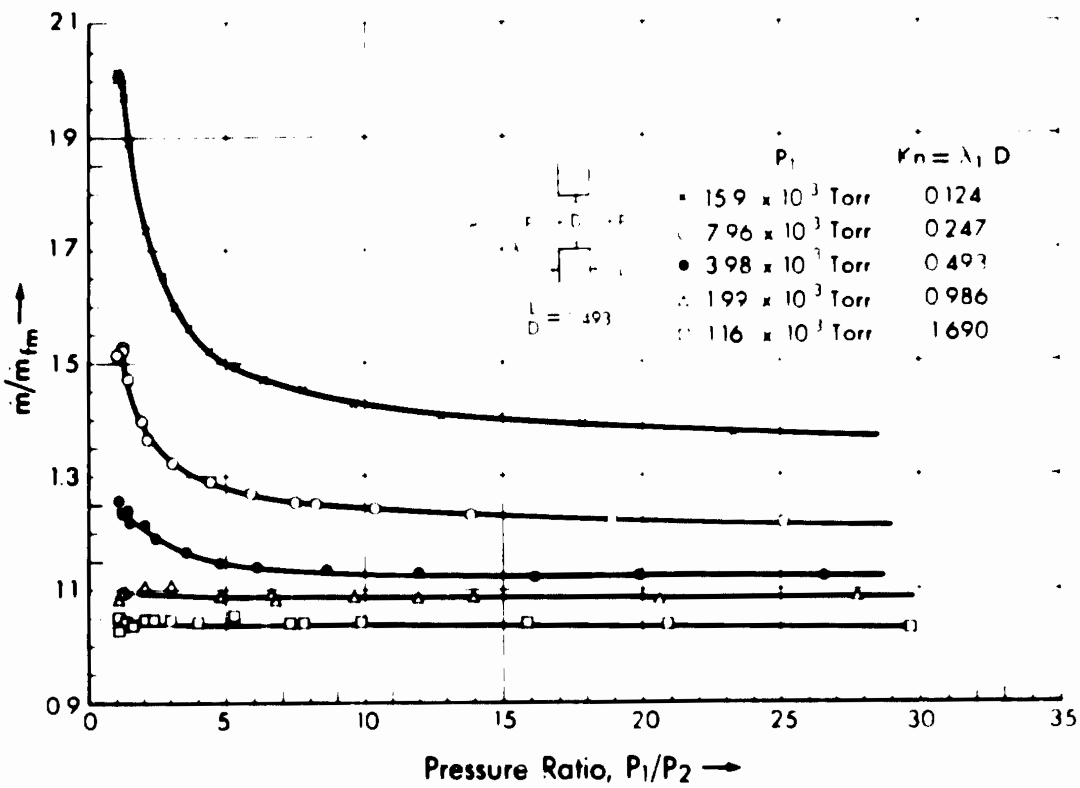

Figure 9. Nondimensionalized mass flow vs pressure ratio at various Knudsen numbers for a short tube, $\frac{L}{D}$ = 0.493.

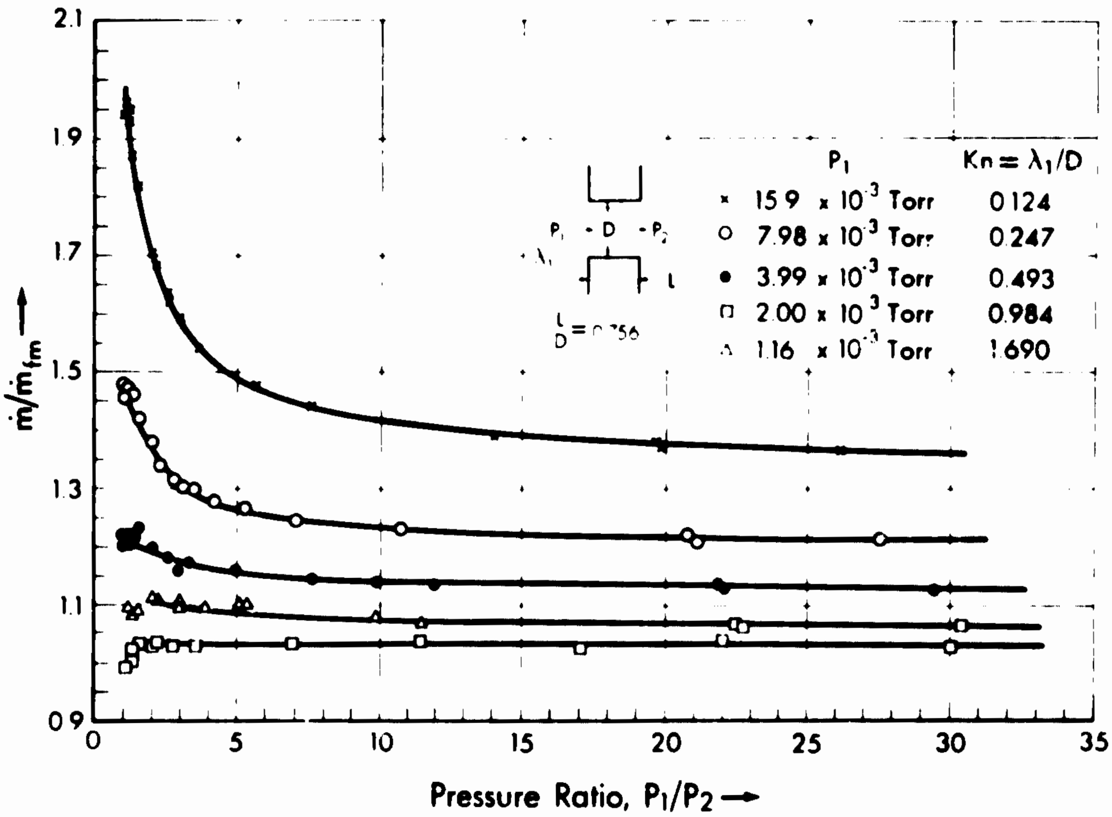

Figure 10. Nondimensionalized mass flow vs pressure ratio at various Knudsen numbers for a short tube, $\frac{L}{D}$ = 0.756.

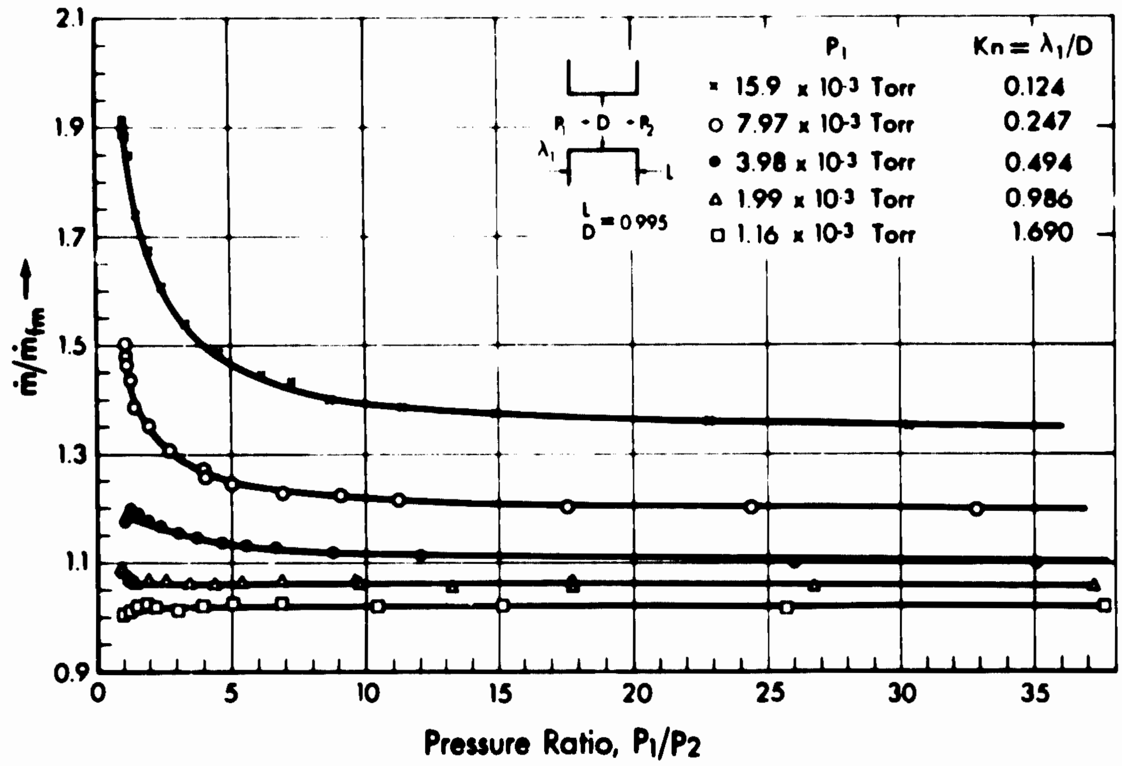

Figure 11. Nondimensionalized mass flow vs pressure ratio at various Knudsen numbers for a short tube, $\frac{L}{D} = 0.995$.

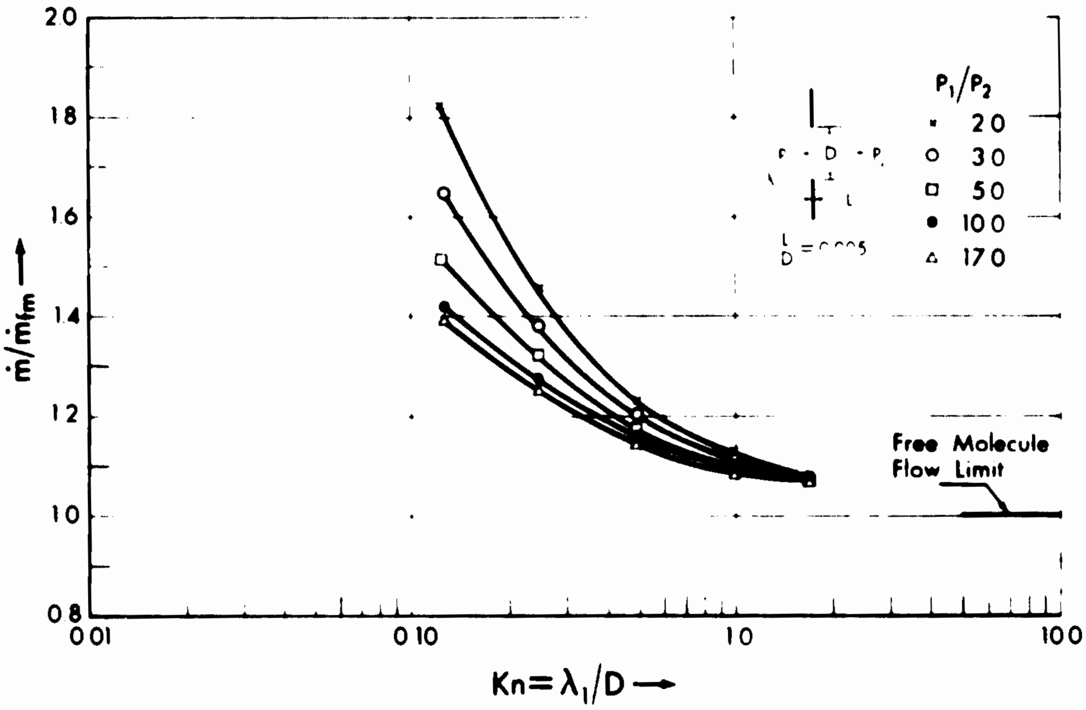

Figure 12. Nondimensionalized mass flow vs Knudsen number at various pressure ratios for an orifice, $\frac{L}{D} = 0.005$.

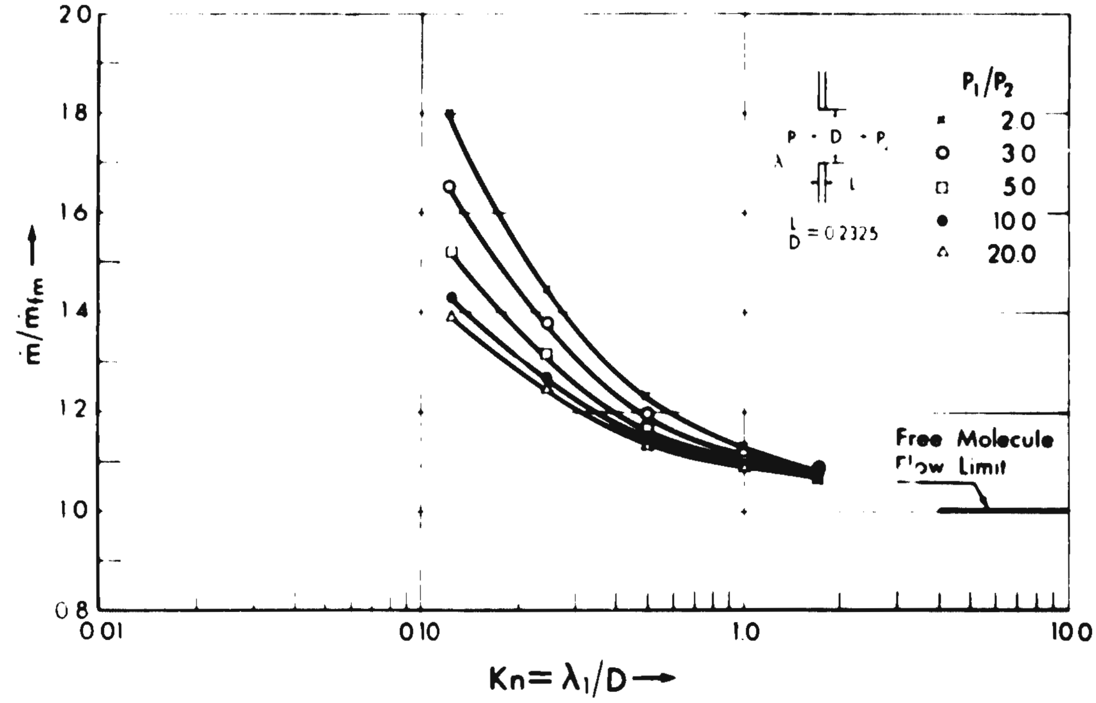

Figure 13. Nondimensionalized mass flow vs Knudsen number at various pressure ratios for a short tube, $\frac{L}{D} = 0.233$.

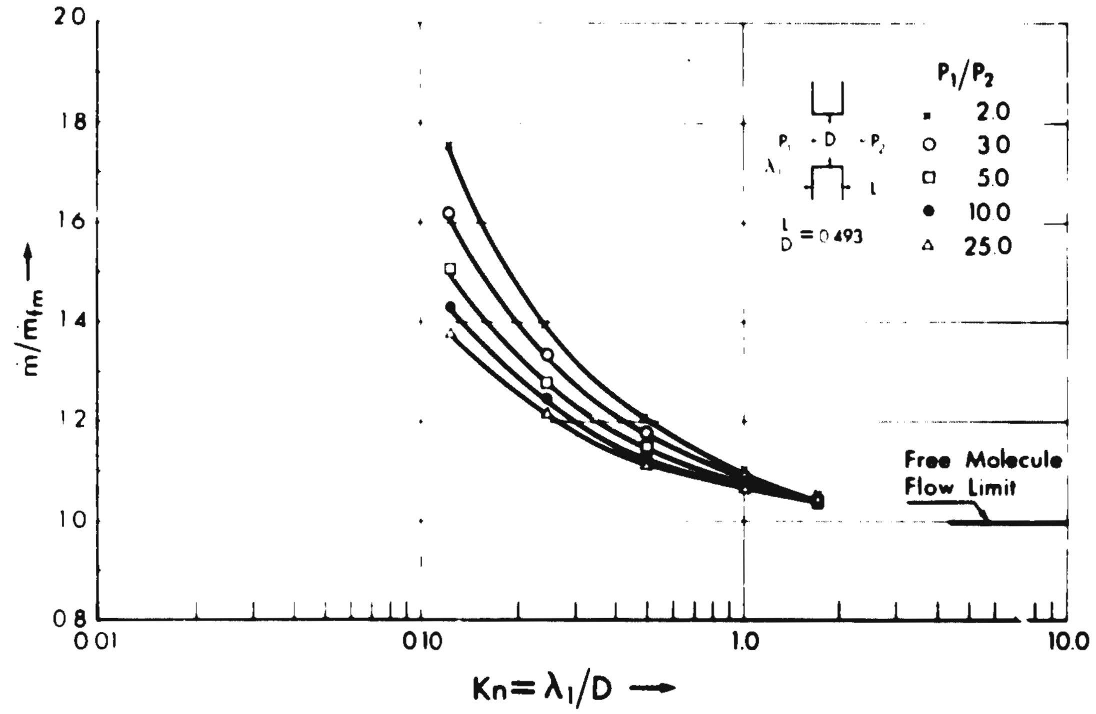

Figure 14. Nondimensionalized mass flow vs Knudsen number at various pressure ratios for a short tube, $\frac{L}{D} = 0.493$.

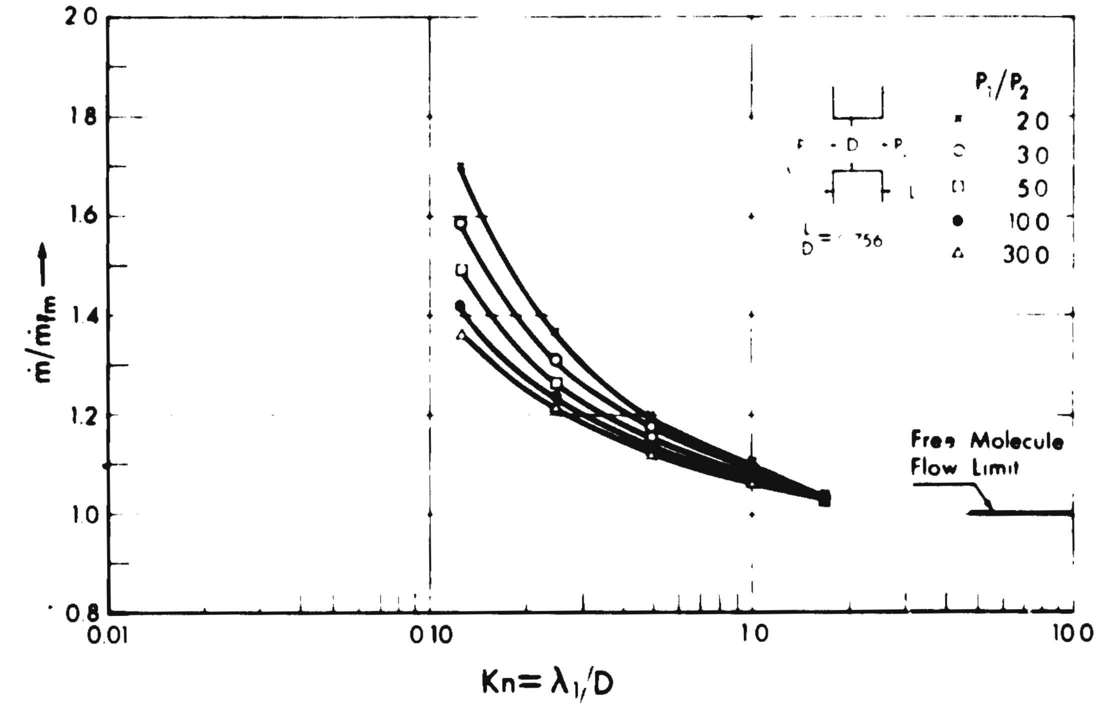

Figure 15. Nondimensionalized mass flow vs Knudsen number at various pressure ratios for a short tube, $\frac{L}{D}$ = 0.756.

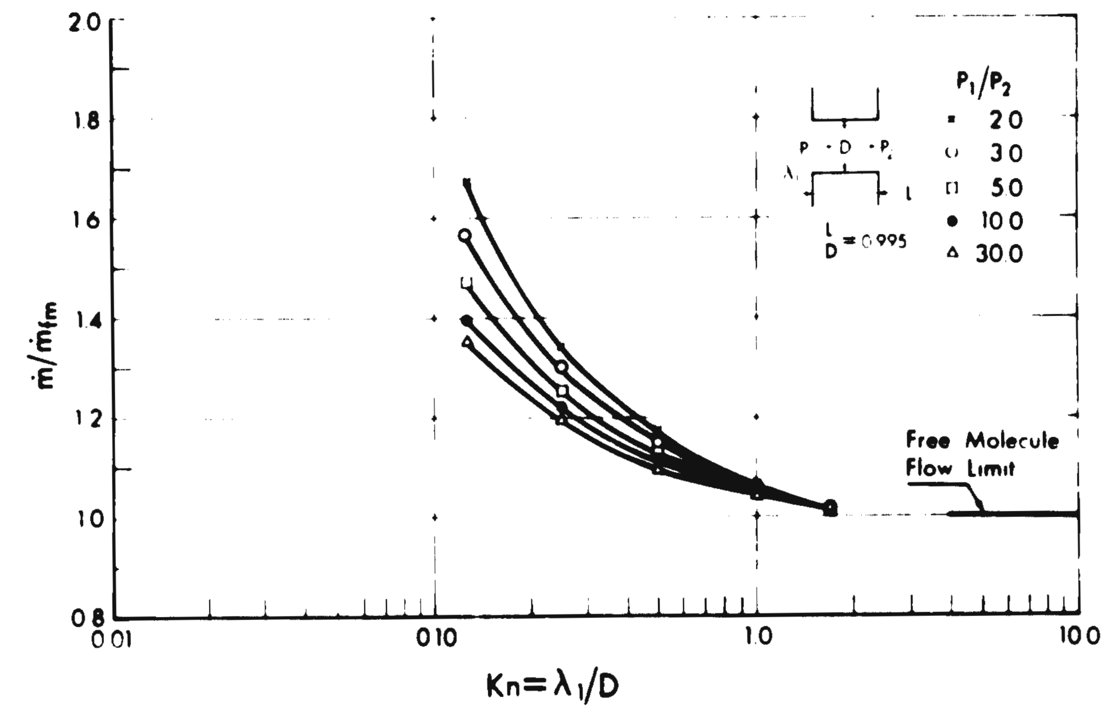

Figure 16. Nondimensionalized mass flow vs Knudsen number at various pressure ratios for a short tube, $\frac{L}{D}$ = 0.995.

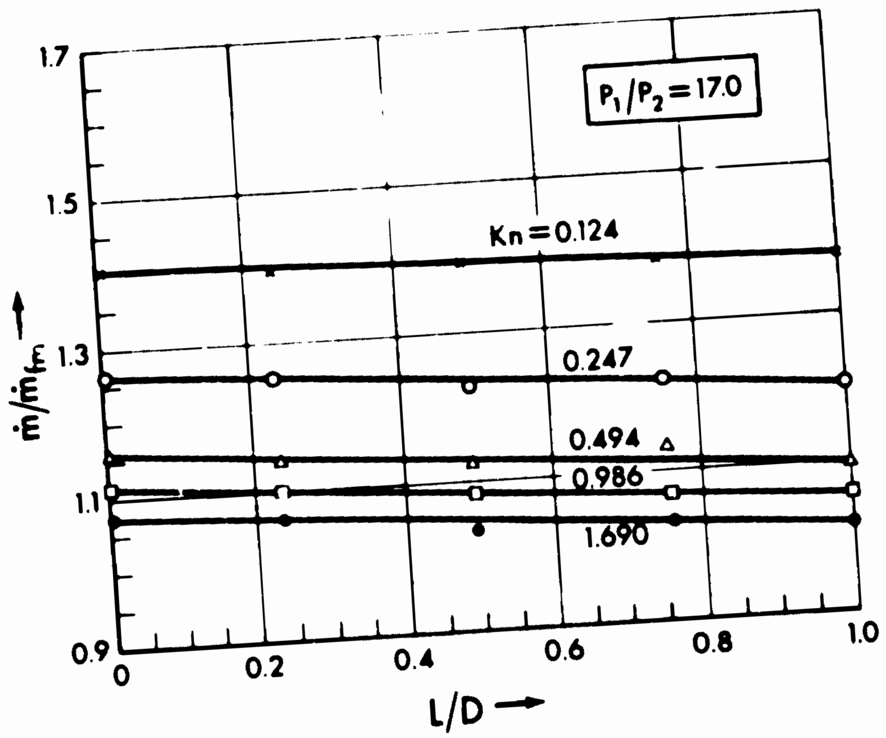

Figure 17. Nondimensionalized mass flow vs length-to-diameter ratio of tubes at various Knudsen numbers at a pressure ratio of 17.

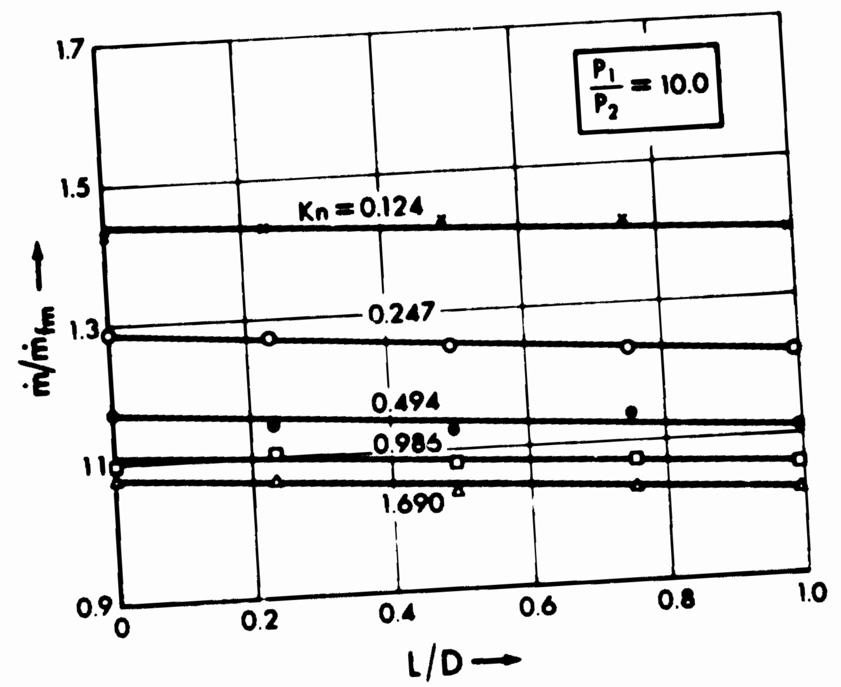

Figure 18. Nondimensionalized mass flow vs length-to-diameter ratio of tubes at various Knudsen numbers at a pressure ratio of 10.

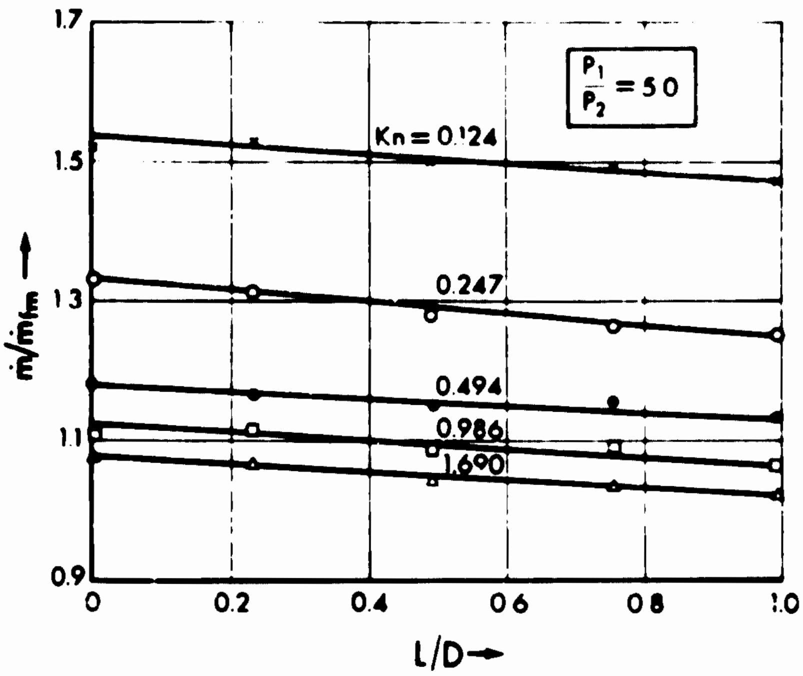

Figure 19. Nondimensionalized mass flow vs length-to-diameter ratio of tubes at various Knudsen numbers at a pressure ratio of 5.

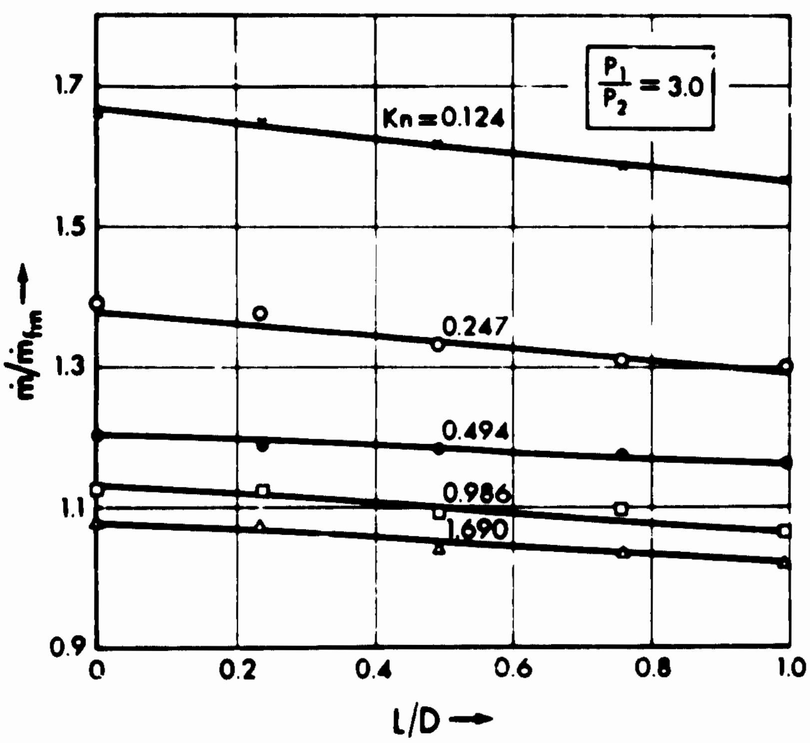

Figure 20. Nondimensionalized mass flow vs length-to-diameter ratio of tubes at various Knudsen numbers at a pressure ratio of 3.

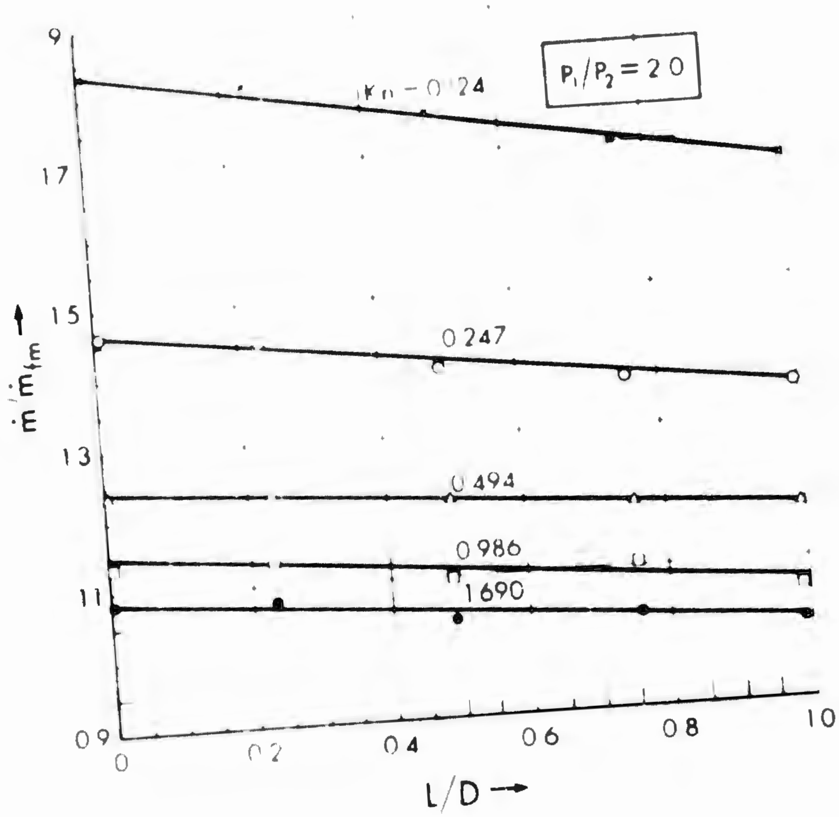

Figure 21. [illegible] flow vs length- [illegible] at various [illegible]

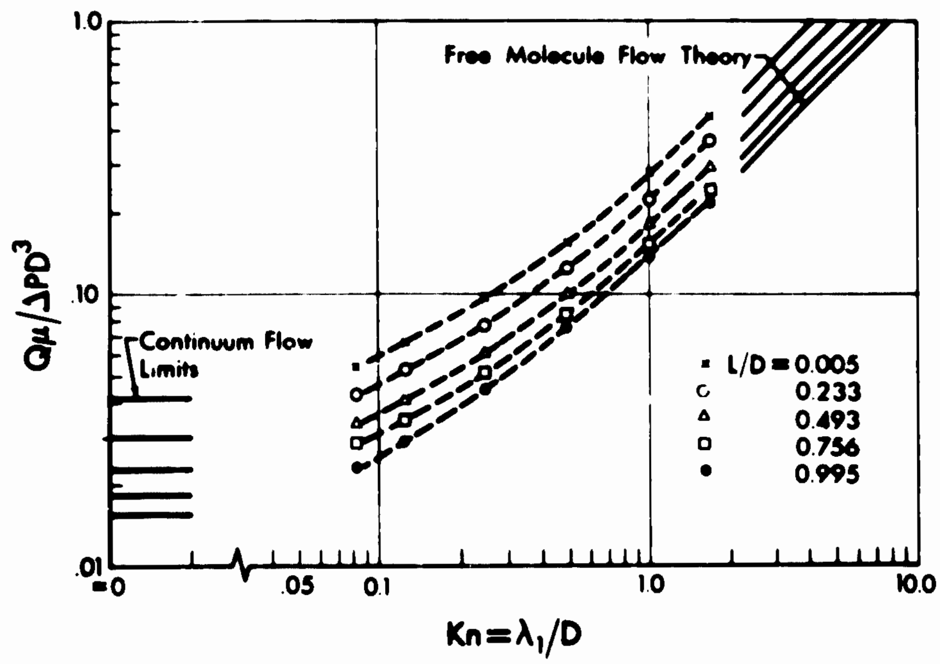

Figure 22. The quantity $\frac{Q\mu}{\Delta PD^3}$ as a function of Knudsen number for small pressure ratios, $\frac{P_1}{P_2} \leqslant 1.2$.

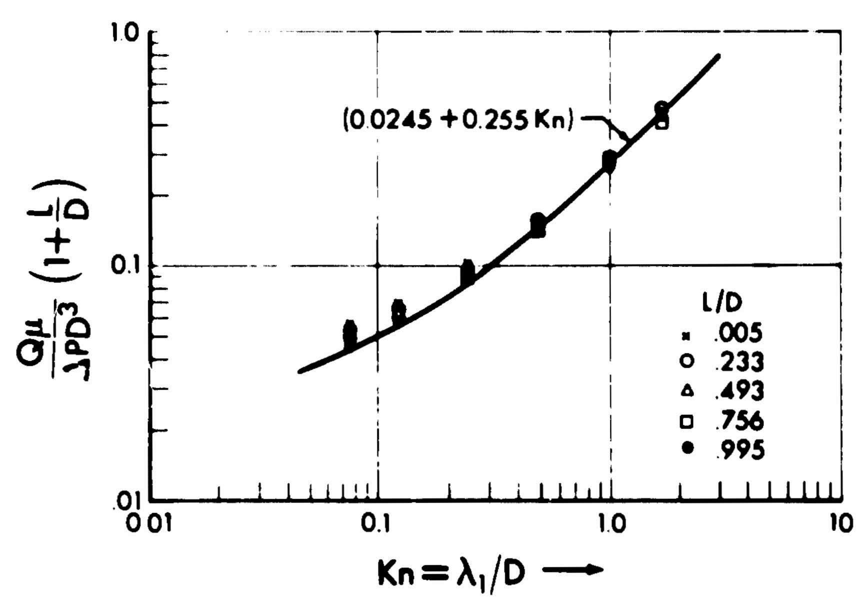

Figure 23. Comparison of the measured data with the semi-empirical equation (8) at small pressure ratios $\frac{P_1}{P_2} \leqslant 1.2$.

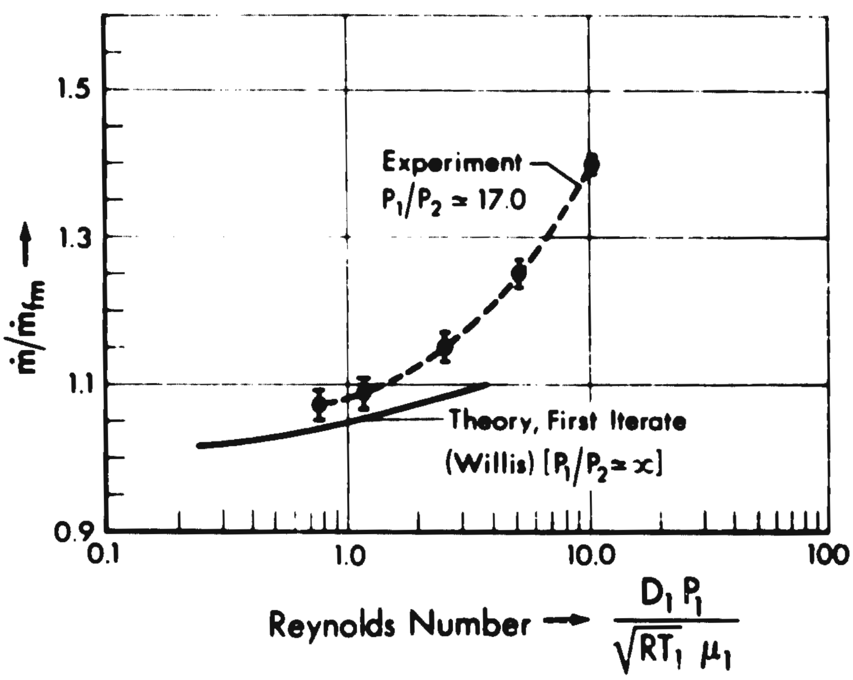

Figure 24. Comparison between theory and experiment of the nondimensionalized mass flows vs Reynolds number for the case of a thin orifice.

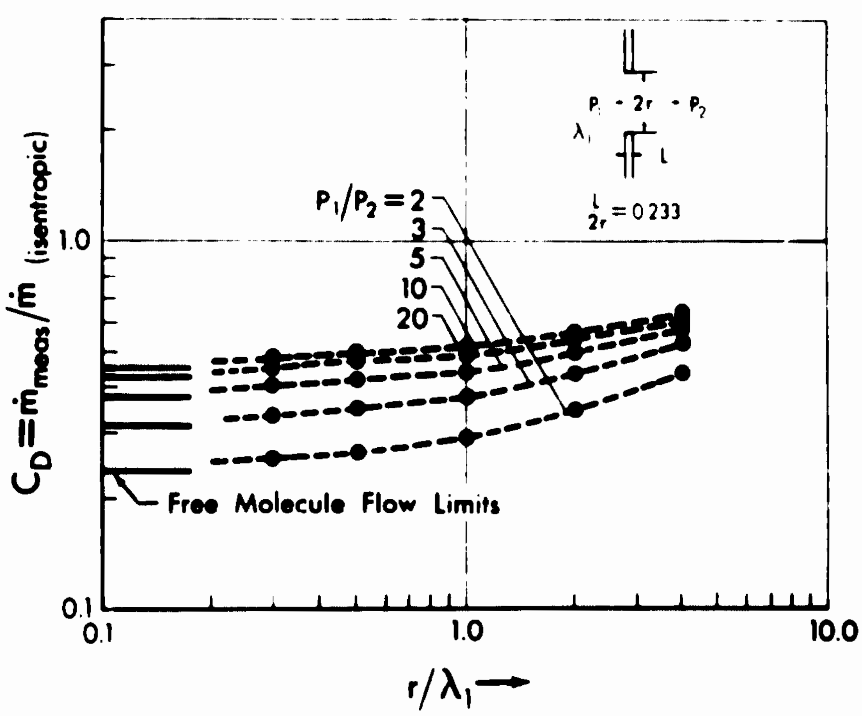

Figure 25. Discharge coefficient, C_D vs inverse of Knudsen number (based on radius) for a tube of $\frac{L}{D}$ = 0.233 at various pressure ratio conditions.

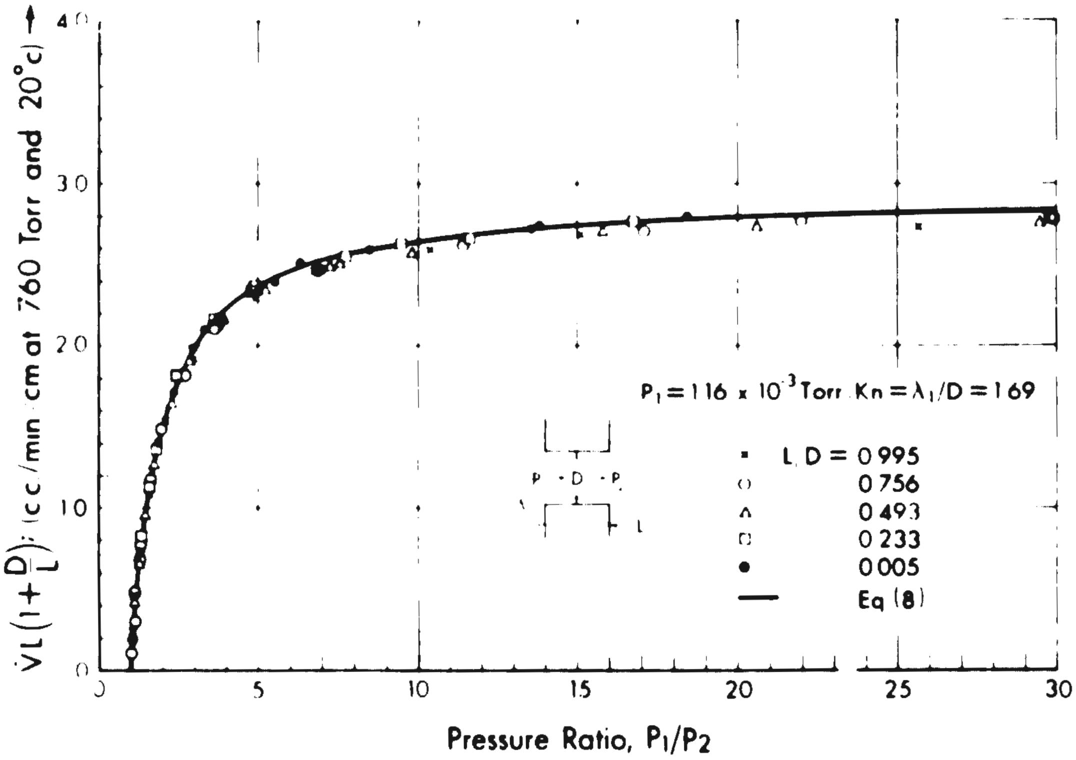

Figure 26. Comparison of the measured flow rate for various tube geometries at a Knudsen number of 1.69 with the semi-empirical equation (8).

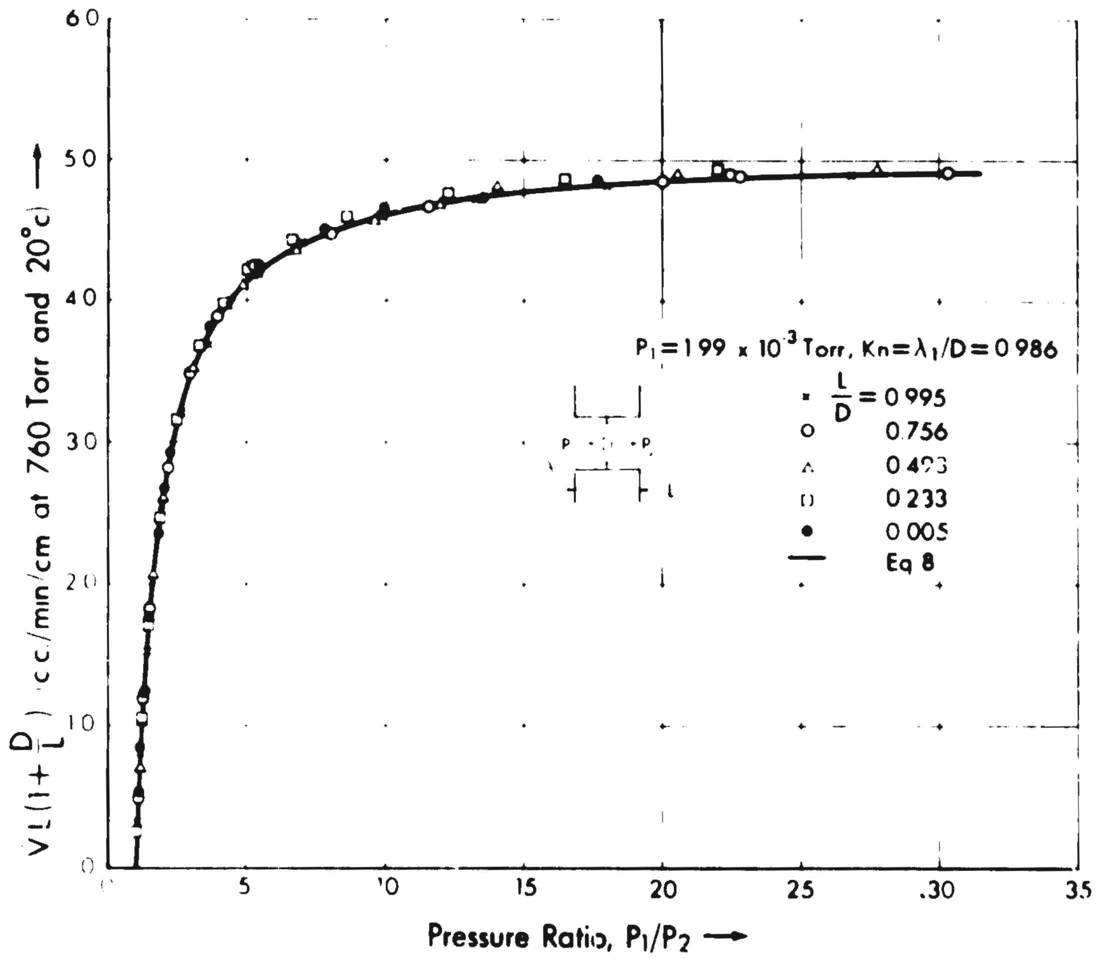

Figure 27. Comparison of the measured flow rate for various tube geometries at a Knudsen number of 0.986 with the semi-empirical equation (8).

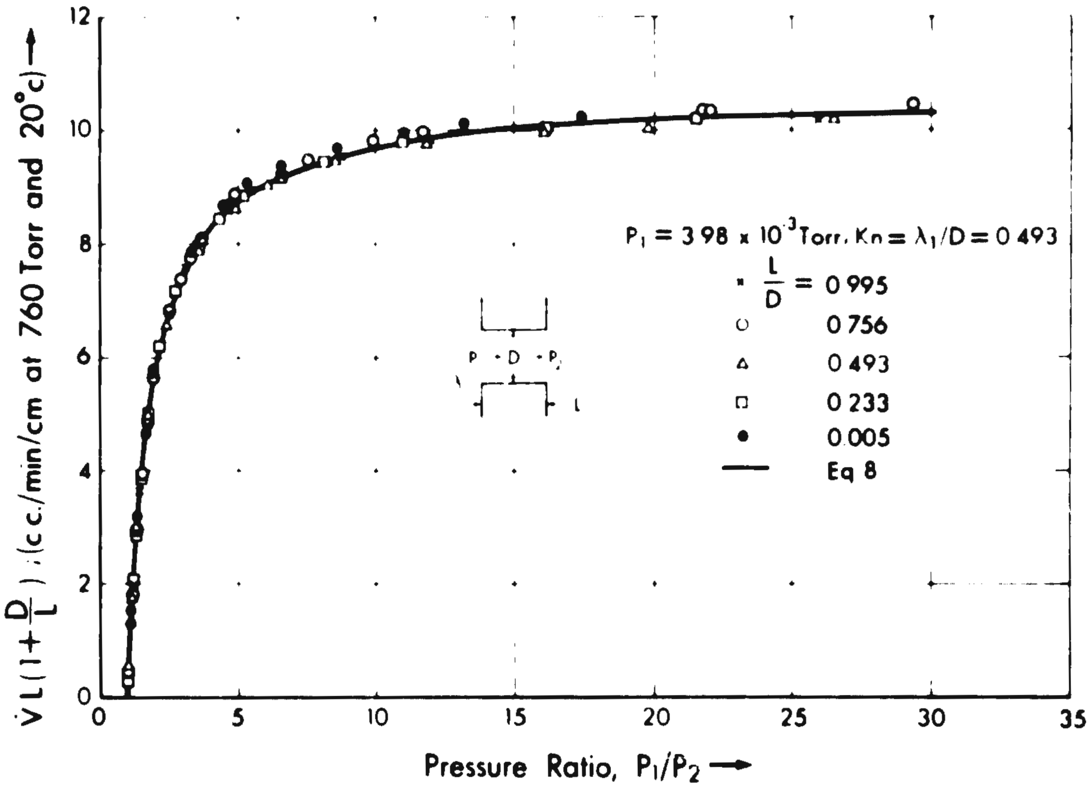

Figure 28. Comparison of the measured flow rate for various tube geometries at a Knudsen number of 0.494 with the semi-empirical equation (8).

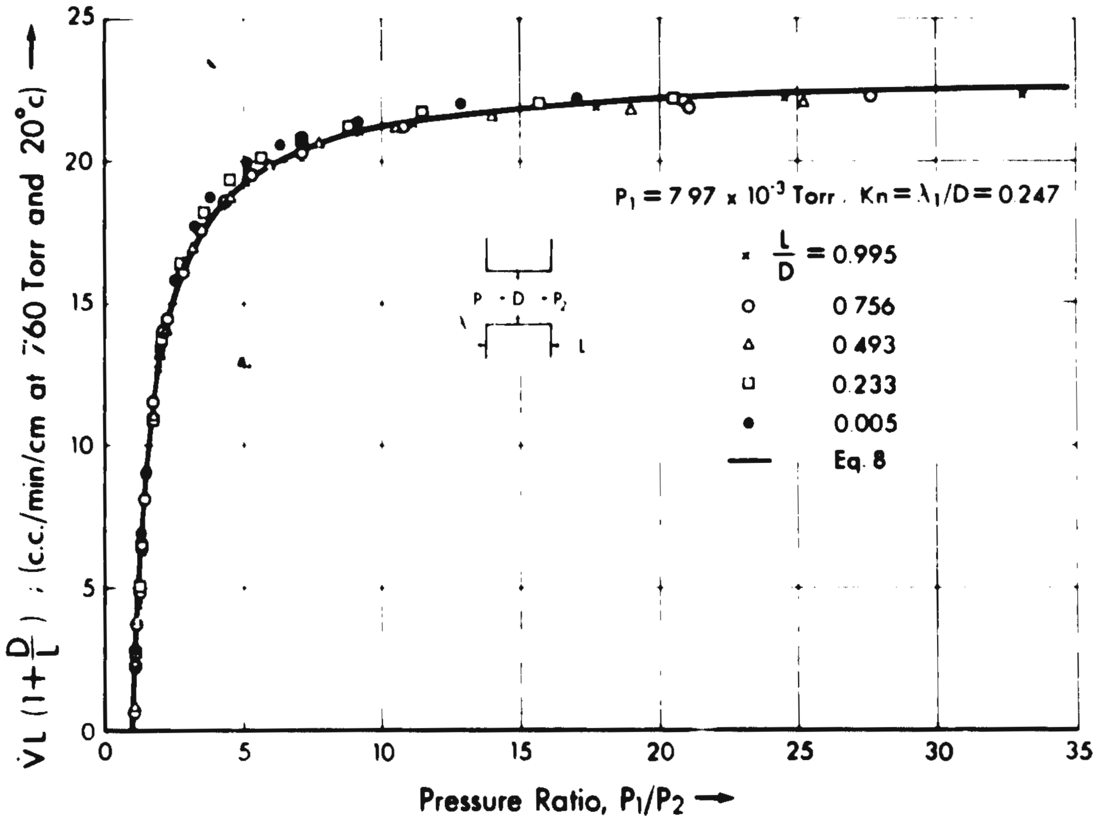

Figure 29. Comparison of the measured flow rate for various tube geometries at a Knudsen number of 0.247 with the semi-empirical equation (8).

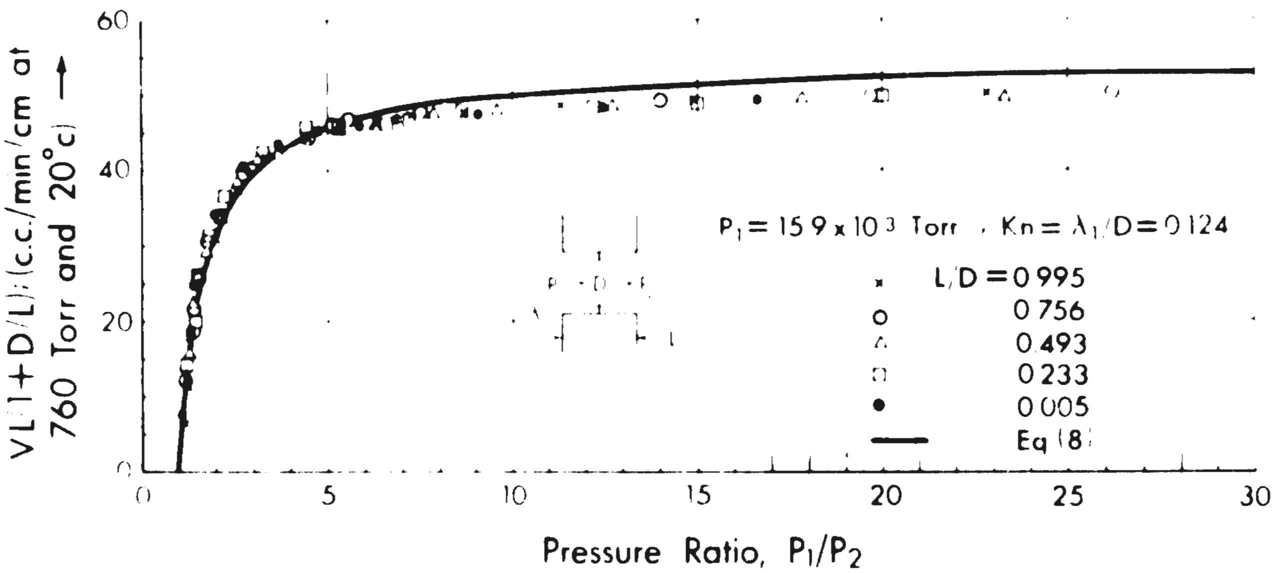

Figure 30. Comparison of the measured flow rate for various tube geometries at a Knudsen number of 0.124 with the semi-empirical equation (8).

V. CONCLUSIONS

The mass flow through short tubes has been measured for the range of pressure ratios from 1 to 20 in the transition flow regime. The Knudsen numbers based on diameter varied from 0.1 to 1.7. For the case of creeping flow, the pressure drop is linearly proportional to volumetric flow as predicted by both continuum and free molecule flow theories (for fixed Kn). The slope of Q vs. ΔP was a function of Knudsen number and length-to-diameter ratio of tubes, and the results show a very smooth transition from the constant continuum value to a linear function of Knudsen number in free molecule flow. At high pressure ratios, for Reynolds number around one, the measured values are slightly higher than Willis' first iterate solution, for the case of an orifice. The mass flows were highly dependent on the pressure ratios for a given tube geometry and pressure ratios greater than 30 are required before it becomes constant for a given upstream condition. For a given upstream pressure, the decrease in the mass flow as the tube length, L, is increased (for fixed diameter, D, of the tube) was found to be proportional to L(1+D/L). A semi-empirical equation was developed to predict the mass flow through short tubes, and this equation is identical to Poiseuille equation with slip boundary conditions multiplied by a factor which is a function of tube geometry alone. This equation was found to be valid at all of the pressure ratios and Knudsen numbers covered in the present experiments. At high Knudsen numbers, the experiments showed that the measurements were approaching asymptotically the theoretical values predicted by Clausing for short tubes.

BLANK PAGE

REFERENCES

1. F. O. Smetana, A.S.M.E. Paper 63-WA-94 (1963).

2. M. W. Milligan, AIAA Journal 2, 6, 1088 (1964).

3. H. Cook and E. A. Richley, NASA TN D-2480 (1964).

4. H. Liepmann, Jour. of Fluid Mech. 10, 1, 65 (1961).

5. A. K. Sreekanth, Proc. of Fourth International Symp. on Rarefied Gas Dynamics (1964) to be published by Academic Press; also Boeing Document D1-82-0322 (1963).

6. W. C. Demarcus, AEC Report K-1302, Part III (1956).

7. R. Roscoe, Phil. Mag. (Ser. 7) 40, 338 (1949).

8. H. L. Weissberg, Phys. of Fluids 5, 9, 1033 (1962).

9. D. R. Willis, Jour. of Fluid Mechanics 21, 1, 21 (1965).

10. R. D. Present, Kinetic Theory of Gases, McGraw-Hill (1958).

ACKNOWLEDGEMENT

The author would like to express his thanks to Dr. H. Harrison and R. Goldstein for reviewing the manuscript, and to Mr. R. Bowey for his help in conducting the experiments.

NOTATION

A	=	cross-sectional area of tube or orifice
$\bar{c}$	=	average molecular speed
D	=	diameter of the tube or orifice
k	=	Clausing factor
Kn	=	Knudsen number, $= \frac{1}{D}$
L	=	length of tube or orifice
$\dot{m}_{fm}$	=	theoretical free molecule mass flow $\left(= \frac{\rho \bar{c}}{4} A\right)$
$\dot{m}_{meas}$	=	measured mass flow
P_1	=	upstream pressure
P_2	=	downstream pressure
$\bar{P}$	=	$\frac{P_1 + P_2}{2}$
ΔP	=	pressure drop across the tube or orifice, $(P_1 - P_2)$
Q	=	volumetric flow at pressure P_1 and temperature T_1
R	=	gas constant
R_e	=	Reynolds number, $= \frac{D P_1}{\sqrt{RT_1}\, \mu_1}$
T_1	=	upstream temperature $\simeq 22.5^{\circ}C$
$\dot{V}_{fm}$	=	theoretical free molecule volumetric flow

$\dot{V}_{meas}$ = measured volumetric flow

γ = ratio of specific heats

λ_1 = upstream mean free path; $\lambda(\text{cms}) = \frac{4.992}{P_1(\text{microns})}$

μ_1 = viscosity of nitrogen at $22.5^{\circ}C$ = 1760.37×10^{-7} poise

(Subscript 1 refers to upstream conditions.)

TABLE 2

P_1 15.91 x 10^{-3} Torr; T_1 22.5 °C; λ_1 0.314 cms; L 0.0127 cm;

D = 2.54 cm; Kn $\frac{\lambda_1}{D}$ 0.124; $\frac{L}{D}$ 0.005.

P_1/P_2	P_2 x 10^{-3} Torr	(cc/min at 760 Torr & 20 °C) $\dot{V}_{fm}$ Theory	$\dot{V}_{meas}$	$\frac{\dot{m}_{meas}}{\dot{m}_{fm}}$
1.126	14.13	8.302	17.92	2.158
1.081	14.72	5.550	12.21	2.199
12.50	1.273	68.28	96.14	1.407
16.61	0.958	69.72	98.00	1.407
9.09	1.750	66.04	94.98	1.438
6.95	2.289	63.52	93.26	1.468
5.823	2.732	61.47	91.80	1.493
4.740	3.356	58.53	89.69	1.532
3.658	4.349	53.92	86.09	1.596
2.790	5.702	47.62	79.92	1.678
2.780	5.723	47.52	79.92	1.682
2.190	7.264	40.35	71.90	1.782
1.800	8.838	32.98	62.06	1.882
1.508	10.550	25.00	49.99	1.999
1.323	12.030	18.09	38.09	2.105
1.213	13.120	13.02	28.09	2.157
1.152	13.81	9.793	21.46	2.190

TABLE 3

P_1 7.955 x 10^{-3} Torr; T_1 22.5°C; λ_1 0.6275 cm; L 0.0127 cms;

D 2.54 cm; Kn $\frac{\lambda_1}{D}$ 0.247; $\frac{L}{D}$ 0.005.

P_1/P_2	P_2 x 10^{-3} Torr	(cc/min at 760 Torr & 20°C) $\dot{V}_{fm}$ Theory	$\dot{V}_{meas}$	$\dot{m}_{meas}/\dot{m}_{fm}$
1.032	7.562	1.833	3.118	1.701
1.084	7.339	2.873	4.815	1.676
1.124	7.077	4.095	6.808	1.662
1.200	6.629	6.184	9.985	1.614
1.276	6.234	8.026	12.670	1.578
1.437	5.536	11.280	17.35	1.537
1.009	7.884	0.330	0.660	1.997
1.040	7.649	1.427	2.22	1.555
1.084	7.339	2.873	4.68	1.629
1.144	6.954	4.668	7.54	1.614
1.144	6.954	4.668	7.53	1.612
1.220	6.520	6.693	10.57	1.578
1.321	6.022	9.016	13.97	1.549
1.436	5.540	11.270	17.17	1.524
17.040	0.467	34.92	44.01	1.260
12.80	0.621	34.21	43.66	1.276
12.87	0.618	34.21	43.61	1.274
9.03	0.881	32.99	42.40	1.285
6.27	1.269	31.18	40.77	1.307
7.09	1.122	31.87	41.53	1.303
5.02	1.585	29.71	39.59	1.332
3.69	2.156	27.05	37.01	1.368
3.187	2.496	25.46	35.18	1.381
2.463	3.230	22.03	31.37	1.424
1.942	4.096	18.00	26.48	1.471
1.652	4.815	14.65	22.10	1.508
1.450	5.486	11.51	17.82	1.547

TABLE 4

P_1 3.98 x 10^{-3} Torr; T_1 22.5°C; λ_1 1.254 cms: L 0.0127 cm;

D 2.54 cm; Kn $\frac{\lambda_1}{D}$ 0.494; $\frac{L}{D}$ 0.005.

P_1/P_2	P_2 x 10^{-3} Torr	(cc/min at 760 Torr & 20°C) $\dot{V}_{fm}$ Theory	$\dot{V}_{meas}$	$\frac{\dot{m}_{meas}}{\dot{m}_{fm}}$
4.680	0.850	14.60	17.19	1.178
3.332	1.194	13.00	15.55	1.196
2.360	1.686	10.70	13.06	1.221
2.000	1.990	9.281	11.47	1.235
1.670	2.383	7.448	9.307	1.250
1.029	3.868	5.224	0.640	1.225
1.050	3.790	8.861	1.110	1.253
1.085	3.668	1.455	1.920	1.319
1.144	3.479	2.337	2.99	1.279
1.200	3.317	3.092	3.999	1.293
1.360	2.926	4.916	6.378	1.297
13.31	0.299	17.17	19.98	1.163
13.24	0.301	17.16	19.98	1.164
17.46	0.228	17.50	20.26	1.157
8.64	0.461	16.41	19.15	1.166
11.10	0.359	16.89	19.68	1.165
5.40	0.737	15.13	17.90	1.184
6.60	0.603	15.75	18.58	1.180
4.50	0.884	14.44	17.14	1.187

TABLE 5

P_1 = 1.993 x 10^{-3} Torr; T_1 = 22.5°C; λ_1 = 2.505 cms; L = 0.0127 cm;

D = 2.54 cm; Kn = $\frac{\lambda_1}{D}$ = 0.986; $\frac{L}{D}$ = 0.005.

P_1/P_2	P_2 x 10^{-3} Torr	(cc/min at 760 Torr & 20°C) $\dot{V}_{fm}$ Theory	$\dot{V}_{meas}$	$\frac{\dot{m}_{meas}}{\dot{m}_{fm}}$
3.030	0.658	6.226	7.04	1.130
2.210	0.902	5.088	5.79	1.137
1.770	1.126	4.043	4.64	1.147
1.484	1.343	3.031	3.45	1.138
1.294	1.540	2.113	2.41	1.140
1.186	1.680	1.460	1.65	1.129
1.115	1.787	0.960	1.10	1.145
1.076	1.852	0.658	0.71	1.079
1.040	1.916	0.359	0.41	1.141
13.50	0.148	8.604	9.41	1.093
17.66	0.113	8.769	9.614	1.096
7.80	0.256	8.100	8.958	1.105
13.55	0.147	8.609	9.455	1.098
5.495	0.363	7.602	8.429	1.108
3.604	0.553	6.717	7.557	1.125
3.027	0.658	6.226	7.034	1.129
11.830	0.168	8.512	9.350	1.098

TABLE 6

P_1 1.163 x 10^{-3} Torr; T_1 22.5°C; λ_1 4.292 cms; L 0.0127 cms;

D 2.54 cms; Kn $\frac{\lambda_1}{D}$ 1.690; $\frac{L}{D}$ 0.005.

P_1/P_2	P_2 x 10^{-3} Torr	(cc/min at 760 Torr & 20°C) $\dot{V}_{fm\ Theory}$	$\dot{V}_{meas}$	$\frac{\dot{m}_{meas}}{\dot{m}_{fm}}$
1.062	1.095	0.318	0.35	1.099
1.176	0.989	0.811	0.90	1.110
1.310	0.888	1.284	1.42	1.106
1.569	9.741	1.970	2.12	1.075
1.880	0.619	2.338	2.79	1.099
2.350	0.495	3.115	3.37	1.082
2.983	0.390	3.603	3.912	1.086
13.66	0.085	5.028	5.401	1.074
8.516	0.137	4.785	5.143	1.075
5.64	0.206	4.463	4.825	1.081
3.94	0.295	4.048	4.36	1.077
18.40	0.063	5.130	5.49	1.071
13.60	0.086	5.023	5.40	1.075
9.71	0.120	4.865	5.27	1.084
6.39	0.182	4.575	4.96	1.083
18.50	0.063	5.130	5.54	1.079
13.81	0.084	5.033	5.43	1.079
3.37	0.345	3.815	4.15	1.087

TABLE 7

$P_1 = 23.85 \times 10^{-3}$ Torr; $T_1 = 22.5^oC$; $\lambda_1 = 0.209$ cm; $L = 0.0127$ cms;
$D = 2.54$ cm; $Kn = \frac{\lambda_1}{D} = 0.0824$; $\frac{L}{D} = 0.005$.

P_1/P_2	P_2 x 10^{-3} Torr	(cc/min at 760 Torr & 20^oC) $\dot{V}_{fm}$ Theory	$\dot{V}_{meas}$	$\frac{\dot{m}_{meas}}{\dot{m}_{fm}}$
1.011	23.59	1.212	4.214	3.476
1.056	22.59	5.877	16.56	2.817
1.235	19.31	21.18	56.24	2.655
1.172	20.35	16.32	44.34	2.717
1.117	21.35	11.66	32.97	2.826

TABLE 8

P_1 15.88 x 10^{-3} Torr; T_1 22.5°C; λ_1 0.3143 cms; L 0.5906 cms;
D 2.54 cm; Kn $\frac{\lambda_1}{D}$ 0.1237; $\frac{L}{D}$ 0.2325.

P_1/P_2	P_2 x 10^{-3} Torr	(cc/min at 760 Torr & 20°C) $\dot{V}_{fm}$ Theory	$\dot{V}_{meas}$	$\frac{\dot{m}_{meas}}{\dot{m}_{fm}}$
1.157	13.725	8.187	17.156	2.095
1.100	14.44	5.483	11.69	2.132
1.063	14.94	3.580	7.803	2.180
15.00	1.06	56.43	79.29	1.405
19.99	0.794	57.46	79.92	1.391
12.24	1.297	55.52	78.28	1.410
8.611	1.844	53.46	77.43	1.448
7.23	2.196	52.09	76.52	1.469
6.404	2.479	51.03	75.62	1.482
5.22	3.042	48.89	74.01	1.514
4.09	3.880	45.70	71.28	1.560
4.03	3.940	45.47	71.11	1.564
3.31	4.80	42.19	68.37	1.621
2.738	5.80	38.38	64.47	1.680
2.29	6.93	34.08	59.35	1.741
1.835	8.653	27.53	51.06	1.855
1.535	10.35	21.06	41.23	1.958
1.362	11.66	16.07	32.42	2.017
1.228	12.93	11.23	23.26	2.071
1.176	13.50	9.06	18.86	2.081

TABLE 9

P_1 7.975 x 10^{-3} Torr; T_1 22.5°C; λ_1 = 0.626 cms; L 0.5906 cm;

D = 2.54 cm; Kn $\frac{\lambda_1}{D}$ 0.2464; $\frac{L}{D}$ 0.2325.

P_1/P_2	P_2 x 10^{-3} Torr	(cc/min at 760 Torr & 20°C) $\dot{V}_{fm}$ Theory	$\dot{V}_{meas}$	$\frac{\dot{m}_{meas}}{\dot{m}_{fm}}$
1.010	7.896	0.301	0.450	1.495
1.029	7.750	0.857	1.320	1.540
1.102	7.237	2.810	4.302	1.531
1.159	6.881	4.166	6.632	1.592
1.204	6.624	5.144	8.064	1.568
1.295	6.158	6.919	10.60	1.532
1.661	4.801	12.09	17.73	1.467
15.58	0.512	28.42	35.64	1.254
20.56	0.388	28.89	35.98	1.245
11.46	0.696	27.72	35.07	1.265
8.77	0.909	26.91	34.34	1.276
7.055	1.130	26.06	33.71	1.294
5.608	1.422	24.95	32.616	1.307
4.453	1.791	23.55	31.257	1.327
3.485	2.288	21.66	29.312	1.353
2.673	2.984	19.00	26.416	1.390
2.011	3.966	15.15	21.973	1.450
1.669	4.778	12.17	17.967	1.476

TABLE 10

P_1 3.985 x 10^{-3} Torr; T_1 22.5°C; λ_1 1.253 cm; L 0.5906 cm;

D 2.54 cms; Kn $\frac{\lambda_1}{D}$ 0.4933; $\frac{L}{D}$ 0.2325.

P_1/P_2	P_2 x 10^{-3} Torr	(cc/min at 760 Torr & 20°C) $\dot{V}_{fm}$ Theory	$\dot{V}_{meas}$	$\frac{\dot{m}_{meas}}{\dot{m}_{fm}}$
8.08	0.493	13.30	15.28	1.149
10.96	0.364	13.79	15.79	1.145
16.14	0.247	14.23	16.21	1.139
21.56	0.185	14.47	16.43	1.135
6.64	0.600	12.89	14.87	1.154
5.23	0.762	12.27	14.26	1.162
4.33	0.920	11.67	13.64	1.169
3.54	1.126	10.89	12.85	1.180
2.75	1.449	9.657	11.61	1.202
2.19	1.820	8.244	10.04	1.217
1.75	2.277	6.504	8.08	1.242
1.486	2.682	4.962	6.29	1.268
1.305	3.054	3.545	4.53	1.278
1.204	3.310	2.570	3.29	1.280
1.163	3.426	2.129	2.73	1.282
1.024	3.892	0.354	0.47	1.328
1.033	3.784	0.765	0.96	1.255
1.116	3.571	0.158	2.00	1.266

TABLE 11

P_1 1.992 x 10^{-3} Torr; T_1 22.5°C; λ_1 2.506 cm; L 0.5906 cm;
D 2.54 cms; Kn $\frac{\lambda_1}{D}$ 0.9866; $\frac{L}{D}$ 0.2325.

P_1/P_2	P_2 x 10^{-3} Torr	(cc/min at 760 Torr & 20°C) $\dot{V}_{fm}$ Theory	$\dot{V}_{meas}$	$\frac{\dot{m}_{meas}}{\dot{m}_{fm}}$
1.050	1.897	0.362	0.420	1.160
1.100	1.811	0.689	0.76	1.103
1.173	1.698	1.120	1.29	1.151
1.250	1.594	1.516	1.69	1.115
22.00	0.090	7.243	7.977	1.101
16.50	0.121	7.125	7.855	1.102
12.24	0.163	6.965	7.689	1.104
8.64	0.232	6.702	7.434	1.109
6.607	0.301	6.439	7.141	1.109
5.077	0.392	6.093	6.790	1.114
4.140	0.481	5.754	6.435	1.118
3.337	0.597	5.312	5.963	1.122
2.467	0.807	4.512	5.097	1.130
1.852	1.076	3.488	3.960	1.135
1.469	1.356	2.422	2.739	1.131

TABLE 12

$P_1 = 1.165 \times 10^{-3}$ Torr; $T_1 = 22.5^{\circ}$C; $\lambda_1 = 4.285$ cms; $L = 0.5906$ cm;
$D = 2.54$ cm; $Kn = \frac{\lambda_1}{D} = 1.687$; $\frac{L}{D} = 0.2325$.

P_1/P_2	P_2 $\times 10^{-3}$ Torr	(cc/min at 760 Torr & 20°C) $\dot{V}_{fm}$ Theory	$\dot{V}_{meas}$	$\frac{\dot{m}_{meas}}{\dot{m}_{fm}}$
21.93	0.053	4.234	4.516	1.067
16.80	0.069	4.173	4.448	1.066
11.56	0.101	4.052	4.322	1.067
7.75	0.150	3.865	4.116	1.065
9.50	0.123	3.968	4.253	1.072
4.88	0.239	3.526	3.767	1.068
4.85	0.240	3.522	3.748	1.064
1.08	1.079	0.327	0.360	1.101
1.17	0.996	0.644	0.730	1.133
1.37	0.850	1.200	1.320	1.100
1.60	0.728	1.664	1.790	1.075
1.853	0.629	2.041	2.21	1.083
2.580	0.452	2.715	2.92	1.075
3.706	0.314	3.241	3.478	1.073
4.98	0.234	3.545	3.806	1.074

TABLE 13

$P_1 = 23.71 \times 10^{-3}$ Torr; $T_1 = 22.5^{\circ}C$; $\lambda_1 = 0.2105$ cm; $L = 0.5906$ cm;

$D = 2.54$ cms; $Kn = \frac{\lambda_1}{D} = 0.0829$; $\frac{L}{D} = 0.2325$.

P_1/P_2	P_2 x 10^{-3} Torr	(cc/min at 760 Torr & $20^{\circ}C$) $\dot{V}_{fm}$ Theory	$\dot{V}_{meas}$	$\frac{\dot{m}_{meas}}{\dot{m}_{fm}}$
1.033	22.95	2.894	7.662	2.648
1.128	21.02	10.24	27.774	2.712
1.201	19.74	15.12	39.251	2.596
1.338	17.72	22.81	56.398	2.472

TABLE 14

$P_1 = 15.87 \times 10^{-3}$ Torr; $T_1 = 22.5^{o}C$; $\lambda_1 = 0.3146$ cms; $L = 1.251$ cms;

$D = 2.539$ cms; $Kn = \frac{\lambda_1}{D} = 0.124$; $\frac{L}{D} = 0.4926$.

P_1/P_2	P_2 $\times 10^{-3}$ Torr	(cc/min at 760 Torr & 20°C) $\dot{V}_{fm}$ Theory	$\dot{V}_{meas}$	$\frac{\dot{m}_{meas}}{\dot{m}_{fm}}$
17.87	0.888	47.38	66.09	1.395
12.75	1.245	46.27	65.26	1.410
9.62	1.650	44.98	64.35	1.431
7.72	2.056	43.68	63.45	1.453
6.21	2.556	42.10	62.03	1.473
5.30	2.994	40.74	60.78	1.492
23.35	0.680	48.05	66.06	1.375
4.467	3.553	38.97	59.29	1.521
3.664	4.331	36.50	57.14	1.565
3.167	5.011	34.35	54.99	1.601
2.637	6.018	31.16	51.53	1.654
2.104	7.543	26.34	45.70	1.735
1.761	9.012	21.69	39.41	1.817
1.453	10.922	15.65	29.85	1.907
1.269	12.51	10.63	20.94	1.970
1.184	13.40	7.813	15.33	1.962
1.119	14.18	5.345	10.82	2.024
1.180	13.45	7.654	15.31	2.000
1.094	14.51	4.238	9.002	2.124

TABLE 15

P_1 = 7.955 x 10^{-3} Torr; T_1 = 22.5°C; λ_1 = 0.6275 cms; L = 1.251 cm;
D = 2.539 cm; Kn = $\frac{\lambda_1}{D}$ = 0.247; $\frac{L}{D}$ = 0.4926.

P_1/P_2	P_2 x 10^{-3} Torr	(cc/min at 760 Torr & 20°C) $\dot{V}_{fm}$ Theory	$\dot{V}_{meas}$	$\frac{\dot{m}_{meas}}{\dot{m}_{fm}}$
1.008	7.892	0.1994	0.310	1.555
1.029	7.731	0.7088	1.030	1.453
1.084	7.339	1.949	2.830	1.452
1.154	6.893	3.361	5.171	1.538
1.309	6.077	5.943	8.941	1.504
2.010	3.958	12.65	17.681	1.398
25.11	0.3168	24.17	29.38	1.216
18.87	0.4216	23.84	29.18	1.224
13.84	0.5748	23.35	28.82	1.234
10.33	0.7701	22.74	28.28	1.244
7.486	1.063	21.81	27.39	1.256
5.856	1.358	20.88	26.52	1.270
4.328	1.838	19.36	25.07	1.295
3.092	2.573	17.03	22.58	1.326
2.192	3.629	13.69	18.79	1.373
1.698	4.685	10.35	14.68	1.418

TABLE 16

$P_1 = 3.984 \times 10^{-3}$ Torr; $T_1 = 22.5^{\circ}C$; $\lambda_1 = 1.253$ cms; $L = 1.251$ cms;

$D = 2.539$ cms; $Kn = \frac{\lambda_1}{D} = 0.4934$; $\frac{L}{D} = 0.4936$.

P_1/P_2	P_2 $\times 10^{-3}$ Torr	(cc/min at 760 Torr & 20°C) $\dot{V}_{fm}$ Theory	$\dot{V}_{meas}$	$\frac{\dot{m}_{meas}}{\dot{m}_{fm}}$
26.58	0.1499	12.13	13.61	1.122
19.83	0.2009	11.97	13.43	1.122
16.07	0.2479	11.82	13.29	1.124
11.98	0.3326	11.55	13.02	1.127
8.609	0.4628	11.14	12.64	1.134
6.094	0.6538	10.54	12.05	1.143
4.855	0.8206	10.01	11.52	1.151
3.596	1.108	9.101	10.61	1.165
2.386	1.670	7.322	8.75	1.195
1.746	2.282	5.386	6.594	1.224
1.339	2.975	3.192	3.950	1.238
1.169	3.408	1.823	2.270	1.245
1.108	3.596	1.229	1.52	1.237
1.050	3.794	0.601	0.73	1.214

TABLE 17

$P_1 = 1.994 \times 10^{-3}$ Torr; $T_1 = 22.5^{\circ}C$; $\lambda_1 = 2.504$ cm; $L = 1.251$ cms;

$D = 2.539$ cms; $Kn = \frac{\lambda_1}{D} = 0.9858$; $\frac{L}{D} = 0.4926$.

P_1/P_2	P_2 $\times 10^{-3}$ Torr	(cc/min at 760 Torr & $20^{\circ}C$) $\dot{V}_{fm}$ Theory	$\dot{V}_{meas}$	$\frac{\dot{m}_{meas}}{\dot{m}_{fm}}$
27.72	0.07193	6.082	6.613	1.087
20.53	0.0971	6.003	6.519	1.086
14.00	0.1424	5.860	6.416	1.095
11.93	0.1671	5.781	6.256	1.082
9.635	0.2070	5.655	6.114	1.081
6.790	0.2937	5.379	5.822	1.082
1.044	1.910	0.2658	0.290	1.091
1.114	1.791	0.6424	0.690	1.074
1.156	1.725	0.8512	0.920	1.081
1.325	1.505	1.547	1.68	1.086
1.660	1.201	2.509	2.75	1.096
1.986	1.004	3.133	3.458	1.104
3.056	0.6525	4.245	4.70	1.107
4.823	0.4134	5.002	5.484	1.096
6.624	0.3010	5.357	5.841	1.090

TABLE 18

P_1 = 1.163 x 10^{-3}Torr; T_1 = 22.5°C; λ_1 = 4.2923 cms; L = 1.251 cms;
D = 2.539 cms; Kn = $\frac{\lambda_1}{D}$ = 1.690; $\frac{L}{D}$ = 0.4926.

P_1/P_2	P_2 x 10^{-3}Torr	(cc/min at 760 Torr & 20°C) $\dot{V}_{fm}$ Theory	$\dot{V}_{meas}$	$\frac{\dot{m}_{meas}}{\dot{m}_{fm}}$
29.52	0.03940	3.555	3.671	1.032
20.70	0.05618	3.502	3.632	1.037
15.84	0.07342	3.448	3.584	1.039
9.86	0.1180	3.307	3.448	1.043
7.62	0.1526	3.197	3.322	1.039
7.23	0.1609	3.171	3.293	1.038
5.28	0.2203	2.983	3.127	1.048
3.96	0.2937	2.751	2.860	o.040
2.94	0.3956	2.428	2.540	1.046
2.30	0.5057	2.080	2.180	1.048
1.777	0.6545	1.609	1.680	1.044
1.074	1.083	0.2531	0.260	1.027
1.184	0.9823	0.5718	0.585	1.023
1.306	0.8905	0.8623	0.890	1.032

TABLE 19

$P_1 = 23.71 \times 10^{-3}$ Torr; $T_1 = 22.5^{\circ}C$; $\lambda_1 = 0.2105$ cms; $L = 1.251$ cm; $D = 2.539$ cm; $Kn = \frac{\lambda_1}{D} = 0.083$; $\frac{L}{D} = 0.4926$.

P_1/P_2	P_2 x 10^{-3} Torr	(cc/min at 760 Torr & 20°C) $\dot{V}_{fm}$ Theory	$\dot{V}_{meas}$	$\frac{\dot{m}_{meas}}{\dot{m}_{fm}}$
1.079	21.97	5.506	14.02	2.546
1.166	20.33	10.696	26.46	2.474

TABLE 20

$P_1 = 15.93 \times 10^{-3}$ Torr; $T_1 = 22.5^oC$; $\lambda_1 = 0.3134$ cms; L = 1.920 cm;
D = 2.539 cms; $Kn = \frac{\lambda_1}{D} = 0.124$; $\frac{L}{D} = 0.756$.

P_1/P_2	P_2 x 10^{-3}Torr	(cc/min at 760 Torr & 20°C) $\dot{V}_{fm}$ Theory	$\dot{V}_{meas}$	$\frac{\dot{m}_{meas}}{\dot{m}_{fm}}$
19.70	0.8086	41.04	56.48	1.376
5.13	3.105	34.81	51.81	1.488
5.62	2.834	35.54	52.56	1.479
7.53	2.116	37.49	54.03	1.441
14.00	1.138	40.14	55.75	1.389
19.80	0.805	41.05	56.29	1.371
4.48	3.556	33.58	50.50	1.504
3.55	4.487	31.06	47.94	1.543
2.95	5.400	28.58	45.55	1.594
2.524	6.311	26.11	42.75	1.637
2.541	6.269	26.22	42.56	1.623
2.120	7.514	22.84	38.48	1.685
1.850	8.611	19.86	34.55	1.740
1.580	10.082	15.87	28.67	1.807
1.450	10.986	13.42	24.62	1.834
1.350	11.80	11.21	20.94	1.868
1.240	12.85	8.367	15.94	1.905
1.163	13.70	6.060	11.79	1.945
1.086	14.67	3.422	6.65	1.943
1.283	12.42	9.537	18.00	1.887
1.197	13.31	7.116	13.75	1.932
1.125	14.16	4.804	9.64	2.007
1.094	14.56	3.715	7.47	2.011
26.20	0.08	41.58	56.75	1.365
1.095	14.55	3.751	7.45	1.986

TABLE 21

$P_1 = 7.980 \times 10^{-3}$ Torr; $T_1 = 22.5^oC$; $\lambda_1 = 0.626$ cm; L = 1.920 cm;
D = 2.539 cm; $Kn = \frac{\lambda_1}{D} = 0.247$; $\frac{L}{D} = 0.756$.

P_1/P_2	P_2 x 10^{-3}Torr	(cc/min at 760 Torr & 20^oC) $\dot{V}_{fm}$ Theory	$\dot{V}_{meas}$	$\frac{\dot{m}_{meas}}{\dot{m}_{fm}}$
20.81	0.383	20.62	25.13	1.219
21.00	0.380	20.63	24.98	1.211
7.015	1.138	18.57	23.09	1.243
10.750	0.742	19.64	24.12	1.228
5.223	1.528	17.51	22.14	1.264
4.230	1.887	16.54	21.13	1.277
4.230	1.887	16.54	21.15	1.279
3.430	2.327	15.34	19.90	1.297
2.806	2.844	13.94	18.33	1.315
2.896	2.756	14.18	18.58	1.310
2.300	3.470	12.24	16.38	1.338
1.708	4.672	8.978	12.48	1.389
1.027	7.770	0.570	0.870	1.526
1.084	7.362	1.677	2.49	1.485
1.026	7.778	0.548	0.760	1.387
1.212	6.584	3.789	5.575	1.471
1.427	5.592	6.481	9.263	1.429
1.763	4.526	9.374	13.056	1.392
2.153	3.706	11.60	15.829	1.364
1.148	6.951	2.793	4.204	1.505
20.84	0.383	20.62	25.087	1.217
27.58	0.289	20.87	25.382	1.216

TABLE 22

$P_1 = 3.99 \times 10^{-3}$Torr; $T_1 = 22.5°C$; $\lambda_1 = 1.251$ cms; L = 1.920 cms;

D = 2.539 cm; $Kn = \frac{\lambda_1}{D} = 0.493$; $\frac{L}{D} = 0.756$.

P_1/P_2	P_2 x 10^{-3}Torr	(cc/min at 760 Torr & 20°C) $\dot{V}_{fm}$ Theory	$\dot{V}_{meas}$	$\frac{\dot{m}_{meas}}{\dot{m}_{fm}}$
2.964	1.346	7.176	8.333	1.161
2.540	1.571	6.565	7.768	1.183
1.980	2.015	5.360	6.444	1.202
1.723	2.316	4.543	5.511	1.213
1.512	2.639	3.667	4.477	1.221
1.330	3.000	2.687	3.313	1.233
1.190	3.353	1.729	2.040	1.180
1.181	3.378	1.661	2.02	1.216
1.094	3.647	0.931	1.160	1.246
1.093	3.651	0.920	1.150	1.250
1.045	3.818	0.467	0.550	1.178
3.240	1.231	7.488	8.793	1.174
3.635	1.098	7.849	9.185	1.170
4.960	0.804	8.647	10.04	1.160
7.584	0.526	9.401	10.75	1.143
9.970	0.400	9.743	11.12	1.141
21.87	0.182	10.33	11.71	1.133
11.94	0.334	9.922	11.29	1.137
29.43	0.136	10.46	11.80	1.128
22.01	0.181	10.34	11.66	1.128

TABLE 23

$P_1 = 1.997 \times 10^{-3}$ Torr; $T_1 = 22.5^{\circ}C$; $\lambda_1 = 2.50$ cms; L = 1.920 cm;
D = 2.539 cm; $Kn = \frac{\lambda_1}{D} = 0.984$; $\frac{L}{D} = 0.756$.

P_1/P_2	P_2 $\times 10^{-3}$ Torr	(cc/min at 760 Torr & 20°C) $\dot{V}_{fm}$ Theory	$\dot{V}_{meas}$	$\frac{\dot{m}_{meas}}{\dot{m}_{fm}}$
22.450	0.089	5.178	5.538	1.07
11.500	0.174	4.948	5.300	1.071
9.870	0.202	4.872	5.254	1.078
5.230	0.382	4.383	4.815	1.098
5.160	0.387	4.370	4.796	1.097
3.88	0.515	4.022	4.399	1.094
2.93	0.682	3.569	3.941	1.104
2.93	0.682	3.569	3.921	1.099
2.144	0.931	2.893	3.196	1.105
1.53	1.305	1.878	2.050	1.092
1.300	1.536	1.251	1.360	1.087
1.126	1.774	0.605	0.63	1.041
1.810	1.103	2.426	2.66	1.096
22.75	0.088	5.181	5.529	1.067
30.30	0.066	5.241	5.584	1.065

TABLE 24

$P_1 = 1.163 \times 10^{-3}$Torr; $T_1 = 22.5^oC$; $\lambda_1 = 4.292$; L = 1.920 cm;

D = 2.539; $Kn = \frac{\lambda_1}{D} = 1.690$; $\frac{L}{D} = 0.756$.

P_1/P_2	P_2 x 10^{-3}Torr	(cc/min at 760 Torr & 20°C) $\dot{V}_{fm}$ Theory	$\dot{V}_{meas}$	$\frac{\dot{m}_{meas}}{\dot{m}_{fm}}$
21.98	0.0529	3.012	3.137	1.041
29.97	0.0388	3.051	3.157	1.035
17.10	0.068	2.972	3.059	1.029
11.40	0.102	2.880	2.990	1.038
6.879	0.169	2.698	2.790	1.034
3.778	0.3078	2.320	2.390	1.030
3.684	0.3156	2.299	2.370	1.030
2.710	0.4291	1.992	2.050	1.029
2.042	0.5695	1.609	1.670	1.038
1.667	0.6976	1.262	1.320	1.046
1.348	0.8627	0.814	0.85	1.044
1.037	1.121	0.114	0.105	0.921
1.125	1.034	0.350	0.330	0.943
1.304	0.8918	0.735	0.760	1.034
1.195	0.9732	0.516	0.520	1.008
1.120	1.038	0.339	0.330	0.973

TABLE 25

P_1 = 23.82 x 10^{-3}Torr; T_1 = 22.5°C; λ_1 = 0.2096 cm; L = 1.92 cm;
D = 2.539 cm; Kn = $\frac{\lambda_1}{D}$ = 0.083; $\frac{L}{D}$ = 0.756.

P_1/P_2	P_2 x 10^{-3}Torr	(cc/min at 760 Torr & 20°C) $\dot{V}_{fm}$ Theory	$\dot{V}_{meas}$	$\frac{\dot{m}_{meas}}{\dot{m}_{fm}}$
6.60	3.609	54.85	87.53	1.596
2.29	10.40	36.42	70.01	1.922
3.02	7.887	43.23	77.93	1.803
4.07	5.852	48.77	83.10	1.704
4.67	5.100	50.81	85.18	1.676
1.685	14.14	26.27	55.80	2.124
1.180	20.19	9.852	23.30	2.365
1.088	21.89	5.238	13.11	2.502

TABLE 26

$P_1 = 15.9 \times 10^{-3}$ Torr; $T_1 = 22.5^{\circ}C$; $\lambda_1 = 0.314$ cms; $L = 2.526$ cm;
$D = 2.54$ cm; $Kn = \frac{\lambda_1}{D} = 0.1236$; $\frac{L}{D} = 0.9946$.

P_1/P_2	P_2 $\times 10^{-3}$ Torr	(cc/min at 760 Torr & 20°C) $\dot{V}_{fm}$ Theory	$\dot{V}_{meas}$	$\frac{\dot{m}_{meas}}{\dot{m}_{fm}}$
30.30	0.525	37.16	50.22	1.351
22.87	0.695	36.75	49.97	1.360
14.92	1.066	35.85	49.35	1.377
11.39	1.396	35.06	48.70	1.389
8.64	1.840	33.98	47.72	1.404
7.28	2.184	33.15	47.52	1.433
6.20	2.565	32.23	46.58	1.445
4.49	3.541	29.87	44.42	1.487
3.42	4.649	27.19	41.80	1.537
2.55	6.235	23.36	37.49	1.605
1.92	8.281	18.42	31.08	1.687
1.33	11.95	9.537	17.54	1.839
1.33	11.95	9.537	17.60	1.845
1.18	13.47	5.864	11.28	1.923
1.13	14.07	4.423	8.403	1.900
1.09	14.59	3.174	6.161	1.941

TABLE 27

P_1 = 7.966 x 10^{-3} Torr; T_1 = 22.5°C; λ_1 = 0.6266 cm; L = 2.526 cm;

D = 2.54 cm; Kn = $\frac{\lambda_1}{D}$ = 0.2467; $\frac{L}{D}$ = 0.9946.

P_1/P_2	P_2 x 10^{-3} Torr	(cc/min at 760 Torr & 20°C) $\dot{V}_{fm}$ Theory	$\dot{V}_{meas}$	$\dot{m}_{meas}/\dot{m}_{fm}$
4.071	1.957	14.52	18.44	1.270
2.858	2.787	12.52	16.39	1.309
1.934	4.119	9.298	12.64	1.359
1.282	6.214	4.235	6.171	1.457
1.186	6.717	3.019	4.409	1.460
1.080	7.376	1.426	2.130	1.494
1.031	7.726	0.580	0.840	1,448
32.95	0.242	18.67	22.35	1.197
24.46	0.326	18.47	22.18	1.201
17.66	0.451	18.16	21.87	1.204
11.13	0.716	17.52	21.30	1.216
9.12	0.873	17.14	20.96	1.223
6.94	1.148	16.48	20.30	1.232
5.08	1.568	15.46	19.30	1.249
4.133	1.927	14.60	18.41	1.261

TABLE 28

$P_1 = 3.98 \times 10^{-3}$ Torr; $T_1 = 22.5^{\circ}C$; $\lambda_1 = 1.254$; $L = 2.526$ cm;
$D = 2.54$ cm; $Kn = \frac{\lambda_1}{D} = 0.4937$; $\frac{L}{D} = 0.9946$.

P_1/P_2	P_2 $\times 10^{-3}$ Torr	(cc/min at 760 Torr & $20^{\circ}C$) $\dot{V}_{fm}$ Theory	$\dot{V}_{meas}$	$\frac{\dot{m}_{meas}}{\dot{m}_{fm}}$
26.02	0.153	9.250	10.16	1.098
35.10	0.1134	9.347	10.296	1.101
12.07	0.3297	8.822	9.817	1.113
8.744	0.4552	8.520	9.543	1.120
6.577	0.6051	8.157	9.193	1.127
5.566	0.7151	7.892	8.932	1.132
4.684	0.8497	7.565	8.602	1.137
3.781	1.053	7.075	8.116	1.147
3.137	1.269	6.552	7.575	1.156
2.496	1.595	5.765	6.744	1.170
2.016	1.974	4.849	5.703	1.176
1.705	2.334	3.978	4.748	1.194
1.463	2.720	3.045	3.623	1.190
1.195	3.330	1.571	1.900	1.209
1.127	3.531	1.085	1.290	1.189
1.057	3.765	0.5197	0.620	1.193
1.019	3.906	0.1788	0.230	1.286

TABLE 29

$P_1 = 1.993 \times 10^{-3}$ Torr; $T_1 = 22.5^{o}C$; $\lambda_1 = 2.505$ cm; L = 2.526 cm;
D = 2.54 cm; $Kn - \frac{\lambda_1}{D} = 0.986$; $\frac{L}{D} = 0.9946$.

P_1/P_2	P_2 x 10^{-3} Torr	(cc/min at 760 Torr & 20°C) $\dot{V}_{fm}$ Theory	$\dot{V}_{meas}$	$\frac{\dot{m}_{meas}}{\dot{m}_{fm}}$
37.27	0.054	4.688	4.958	1.058
26.77	0.0745	4.637	4.901	1.057
17.91	0.1113	4.548	4.815	1.059
13.26	0.1503	4.454	4.719	1.059
9.73	0.2048	4.322	4.594	1.063
9.87	0.2019	4.329	4.594	1.061
6.91	0.2884	4.120	4.399	1.068
5.45	0.3657	3.933	4.185	1.064
4.42	0.4509	3.727	3.960	1.063
3.58	0.5567	3.472	3.690	1.063
2.635	0.7564	2.989	3.196	1.069
1.980	1.006	2.386	2.550	1.069
1.418	1.406	1.419	1.520	1.071
1.185	1.682	0.752	0.810	1.077
1.067	1.868	0.302	0.320	1.060

TABLE 30

P_1 = 1.163 x 10^{-3}Torr; T_1 = 22.5°C; λ_1 = 4.292 cms; L = 2.526 cm;
D = 2.54 cms; Kn = $\frac{\lambda_1}{D}$ = 1.690; $\frac{L}{D}$ = 0.9946.

P_1/P_2	P_2 x 10^{-3}Torr	(cc/min at 760 Torr & 20°C) $\dot{V}_{fm}$ Theory	$\dot{V}_{meas}$	$\frac{\dot{m}_{meas}}{\dot{m}_{fm}}$
25.69	0.453	2.701	2.74	1.014
37.62	0.0309	2.736	2.79	1.020
15.11	0.077	2.625	2.68	1.021
10.38	0.112	2.540	2.59	1.020
6.97	0.1668	2.408	2.47	1.026
6.84	0.170	2.400	2.46	1.025
5.02	0.2316	2.251	2.30	1.022
3.94	0.2952	2.097	2.14	1.021
3.69	0.3152	2.049	2.13	1.040
3.08	0.3776	1.898	1.92	1.012
2.15	0.5409	1.504	1.53	1.017
1.604	0.7251	1.058	1.08	1.021
1.280	0.9086	0.6149	0.61	0.992
1.187	0.9798	0.4428	0.45	1.016
1.090	1.067	0.2320	0.23	0.991

TABLE 31

$P_1 = 23.72 \times 10^{-3}$ Torr; $T_1 = 22.5^{\circ}C$; $\lambda_1 = 0.2105$ cm; L = 2.526 cm;

D = 2.54 cm; $Kn = \frac{\lambda_1}{D} = 0.0829$; $\frac{L}{D} = 0.9946$.

P_1/P_2	P_2 $\times 10^{-3}$ Torr	(cc/min at 760 Torr & $20^{\circ}C$) $\dot{V}_{fm}$ Theory	$\dot{V}_{meas}$	$\frac{\dot{m}_{meas}}{\dot{m}_{fm}}$
1.030	23.03	1.668	4.107	2.462
1.152	20.59	7.565	17.31	2.288
1.162	20.41	8.000	17.85	2.232
1.024	23.16	1.354	3.013	2.225
6.720	3.530	48.80	75.86	1.555
8.530	2.781	50.61	76.31	1.508
6.69	3.546	48.75	74.93	1.537
4.03	5.886	43.10	70.49	1.635
2.823	8.402	37.03	64.41	1.739
2.09	11.35	29.90	55.77	1.865
1.630	14.55	22.16	44.15	1.992
1.297	18.29	13.12	28.22	2.151
1.068	22.21	3.65	8.20	2.246

TABLE 32

[Note: P_1 in microns Hg; Q = in cc/sec at Pressure P_1 and Temp T_1; ΔP in dynes/sq cm]

$\frac{L}{D} = 0.005$

P_1	Kn	$\frac{Q}{\Delta P}$	$\frac{Q \mu_1}{\Delta P \ D^3}$
23.85	0.082	5,143	0.05522
15.91	0.124	6,143	0.06597
7.955	0.247	9,215	0.09896
3.980	0.494	14,444	0.1551
1.993	0.986	25,722	0.2762
1.163	1.690	42,431	0.4556

$\frac{L}{D} = 0.2325$

P_1	Kn	$\frac{Q}{\Delta P}$	$\frac{Q \mu_1}{\Delta P \ D^3}$
23.71	0.083	4,041	0.04340
15.88	0.124	4,827	0.05184
7.975	0.246	7,209	0.07741
3.985	0.493	11,806	0.1268
1.992	0.987	20,300	0.2180
1.165	1.690	34,956	0.3754

$\frac{L}{D} = 0.4926$

P_1	Kn	$\frac{Q}{\Delta P}$	$\frac{Q \mu_1}{\Delta P \ D^3}$
23.71	0.083	3,213	0.03450
15.87	0.124	3,834	0.04117
7.955	0.247	5,806	0.06235
3.984	0.493	9,500	0.1020
1.994	0.986	16,483	0.1770
1.163	1.690	27,189	0.2920

TABLE 32 (Continued)

$\frac{L}{D} = 0.7561$

P_1	Kn	$\frac{Q}{\Delta P}$	$\frac{Q\ \mu_1}{\Delta P\ D^3}$
23.82	0.083	2,655	0.02852
15.93	0.124	3,188	0.03424
7.98	0.247	4,803	0.05159
3.99	0.493	7,877	0.08461
1.997	0.984	14,106	0.1515
1.163	1.690	22,493	0.2416

$\frac{L}{D} = 0.9946$

P_1	Kn	$\frac{Q}{\Delta P}$	$\frac{Q\ \mu_1}{\Delta P\ D^3}$
23.72		2,141	0.02299
15.90		2,748	0.02952
7.966		4,282	0.04598
3.980		6,886	0.07394
1.993		12,500	0.1342
1.163		19,979	0.2146